A study of the surface heat budget of the Weddell Sea using a radiative transfer model during the austral winter 1994.

Tramm, Eugene P.

Monterey, California. Naval Postgraduate School

NAVAL POSTGRADUATE SCHOOL
Monterey, California

THESIS

A STUDY OF THE SURFACE HEAT BUDGET OF THE WEDDELL SEA USING A RADIATIVE TRANSFER MODEL DURING THE AUSTRAL WINTER 1994

by

Eugene P. Tramm

March, 1997

Thesis Co-Advisors: Peter S. Guest
Roland W. Garwood

Approved for public release; distribution is unlimited.

DUDLEY KNOX LIBRARY
NAVAL POSTGRADUATE SCHOOL
MONTEREY, CA 93943-5101

REPORT DOCUMENTATION PAGE

Form Approved OMB No. 0704-0188

1. AGENCY USE ONLY *(Leave blank)*	2. REPORT DATE MARCH/1997	3. REPORT TYPE AND DATES COVERED Master's Thesis

4. TITLE AND SUBTITLE A STUDY OF THE SURFACE HEAT BUDGET OF THE WEDDELL SEA USING A RADIATIVE TRANSFER MODEL DURING THE AUSTRAL WINTER 1994	5. FUNDING NUMBERS
6. AUTHOR(S) Tramm, Eugene P.	
7. PERFORMING ORGANIZATION NAME(S) AND ADDRESS(ES) Naval Postgraduate School Monterey CA 93943-5000	8. PERFORMING ORGANIZATION REPORT NUMBER
9. SPONSORING/MONITORING AGENCY NAME(S) AND ADDRESS(ES)	10. SPONSORING/MONITORING AGENCY REPORT NUMBER

11. SUPPLEMENTARY NOTES The views expressed in this thesis are those of the author and do not reflect the official policy or position of the Department of Defense or the U.S. Government.

12a. DISTRIBUTION/AVAILABILITY STATEMENT Approved for public release; distribution is unlimited.	12b. DISTRIBUTION CODE

13. ABSTRACT *(maximum 200 words)*

This study uses rawinsonde soundings and irradiance measurements taken in the Weddell Sea during the 1994 ANZFLUX experiment. A radiative transfer model was used to determine the influence of aerosols, cloud droplet size and water content on the radiative heat budget of the Weddell Sea. The modeled irradiances were compared with observations, and the model calculated the upward longwave irradiance from the Weddell Sea ice pack. Turbulent heat fluxes were calculated and combined with radiative terms to provide a net heat flux at the ice surface. While turbulent heat flux is the major factor affecting the Weddell Sea's heat budget in windy conditions, during calm conditions longwave radiative transfer becomes important. The modeled downward irradiances were compared to results obtained from empirical equations developed for the Weddell Sea during the winter. The atmosphere above the Weddell Sea appears to have an aerosol structure similar to marine environments. Stratus clouds over the Weddell Sea appear to be made up of cloud droplets with an effective radius of 2.5 microns and a water concentration close to 0.05 grams per cubic meter. The dominant terms in the surface heat budget are the longwave irradiances with the upward longwave term being the largest.

14. SUBJECT TERMS WEDDELL SEA, SURFACE HEAT BUDGET, RADIATIVE TRANSFER, TURBULENT HEAT FLUX, AEROSOL CONTENT, CLOUD MICROSTRUCTURE	15. NUMBER OF PAGES 102
	16. PRICE CODE

17. SECURITY CLASSIFICATION OF REPORT Unclassified	18. SECURITY CLASSIFICATION OF THIS PAGE Unclassified	19. SECURITY CLASSIFICATION OF ABSTRACT Unclassified	20. LIMITATION OF ABSTRACT UL

NSN 7540-01-280-5500

Standard Form 298 (Rev. 2-89)
Prescribed by ANSI Std. 239-18 298-102

A STUDY OF THE SURFACE HEAT BUDGET OF THE WEDDELL SEA USING A RADIATIVE TRANSFER MODEL DURING THE AUSTRAL WINTER 1994

Eugene P. Tramm
Lieutenant Commander, United States Navy
B.A., University of Virginia, 1983
B.S., University of La Verne, 1991

Submitted in partial fulfillment
of the requirements for the degrees of

MASTER OF SCIENCE IN METEOROLOGY
MASTER OF SCIENCE IN PHYSICAL OCEANOGRAPHY

from the

NAVAL POSTGRADUATE SCHOOL
March 1997

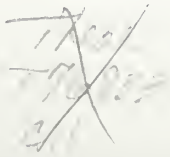

ABSTRACT

This study uses rawinsonde soundings and irradiance measurements taken in the Weddell Sea during the 1994 ANZFLUX experiment. A radiative transfer model was used to determine the influence of aerosols, cloud droplet size and water content on the radiative heat budget of the Weddell Sea. The modeled irradiances were compared with observations, and the model calculated the upward longwave irradiance from the Weddell Sea ice pack. Turbulent heat fluxes were calculated and combined with radiative terms to provide a net heat flux at the ice surface. While turbulent heat flux is the major factor affecting the Weddell Sea's heat budget in windy conditions, during calm conditions longwave radiative transfer becomes important. The modeled downward irradiances were compared to results obtained from empirical equations developed for the Weddell Sea during the winter. The atmosphere above the Weddell Sea appears to have an aerosol structure similar to marine environments. Stratus clouds over the Weddell Sea appear to be made up of cloud droplets with an effective radius of 2.5 microns and a water concentration close to 0.05 grams per cubic meter. The dominant terms in the surface heat budget are the longwave irradiances with the upward longwave term being the largest.

TABLE OF CONTENTS

I. INTRODUCTION

Little is presently known about the factors that control the surface heat budget of the Weddell Sea. Developing an understanding of the surface heat budget is important in understanding the driving mechanisms for small scale mixing processes in the upper ocean. These small scale processes can initiate deep convection events in the Weddell Sea that allow for the transfer of large amounts of heat to the surface. This heat transfer can have significant effects on the surface ice concentration. Changes in the ice concentration of the Weddell Sea can affect the environment on a global scale. Indeed, work by Schlesinger and Mitchell (1985) has shown that changes affecting the ice concentration of the Weddell Sea in the winter may result in significant local atmospheric temperature changes which in turn can lead to a change in temperatures on a global scale.

The stability of the Weddell Sea water column can exist in two different modes that each have distinctive sea ice concentrations and mechanics of deep water formation (Gordon, 1991). A stable mode can exist that supports a coastal deep water formation mechanism and a large areal ice concentration. An unstable mode can exist that can cause very deep convection with strong fluxes of heat and salt. The

large heat flux toward the surface can keep the surface water too warm for ice to form. The amount of deep water formation in the unstable mode can be much greater than that formed during the stable mode. Since the Weddell Sea provides a significant amount of the world's deep/bottom water, events that influence this formation can have a large impact on the world's oceans. To understand how changes in the Weddell Sea ice pack and deep water formation mechanisms occur, a better understanding of the air-ice-sea interface must be developed. Understanding the nature of the factors affecting the surface heat flux at the air-ice-sea interface is a significant part of this problem.

Vertical heat exchange at the ice surface is a function of the incoming solar radiation, radiative fluxes into and out of the ice surface, turbulent heat fluxes, both latent and sensible, and the amount of heat that can be conducted from the ocean upward through the ice. Some of this conducted heat may be lost due to melting or given up due to freezing. Both radiative and turbulent processes contribute to the removal or addition of heat from the surface. However, the turbulent heat fluxes over the ice are usually small compared to the radiation fluxes, especially during the winter. Therefore the longwave surface radiation balance largely controls the surface heat budget of the Weddell Sea in the winter (Guest,

1996).

Intense storm events can cause extremely large localized turbulent heat fluxes into the atmosphere over open water leads in the ice pack. The regional average turbulent heat flux is still quite small however because of the small areal percentage, about 5%, of open water leads in the Weddell Sea ice pack (Guest, 1996). The major mechanism for heat removal during the winter is due to turbulence produced in the upper ocean as storms cause the movement of ice over the ocean (Guest, 1996). This turbulence results in entrainment of heat from below the ocean mixed layer. This extra heat then causes the ice to melt. The heat can then be lost to the atmosphere as upward longwave radiation and sensible heat. Even during periods of relative calm there is still heat being conducted through the ice and lost to the atmosphere due to upward radiative cooling at the ice surface. Guest and Davidson (1994) have shown that the ice can act as a buffer between atmospheric forcing events and temperature changes at the ice surface.

Clouds can have a significant impact on both the radiation reaching the surface and on the amount of radiation allowed to leave the surface. Yamanouchi and Orbaek (1995) have shown how differences in cloud cover can affect the surface radiation budget in both the Arctic and the Antarctic.

Radiative cooling at the surface can create shallow, stable atmospheric boundary layers which allow for the existence of low stratus decks (Guest *et al.*, 1995). These shallow stratus decks can then act to limit the amount of surface heat loss by emitting downward longwave radiation.

An understanding of what factors control radiative processes in the atmosphere is important to gaining an understanding of the surface heat budget at the air-ice-ocean interface. Factors such as airborne aerosols, sub-visible ice crystals or "diamond dust" and cloud macrostructure and microstructure (Curry *et al.*, 1990; Curry and Ebert, 1992) all affect the magnitude and spatial distribution of the surface radiation balance. More work needs to be done to quantify and understand these properties.

The purpose of this study will be to examine the heat flux terms in the surface heat budget of the Weddell Sea and examine atmospheric factors that control the longwave radiation terms. First we will examine more closely some of the factors that control the surface radiative heat budget of the Weddell Sea in winter. Specifically we will examine atmospheric aerosols, cloud droplet size and cloud water concentration. Using a model that simulates the physics of radiative transfer and a data set obtained during the Antarctic Zone Flux Experiment (ANZFLUX), we will attempt to

determine the aerosol structure and cloud microstructure that influence the surface heat budget of the Weddell Sea in the winter. By comparing the modeled downward longwave and shortwave surface irradiances with measured values, we intend to identify properties of the atmospheric aerosols and cloud microstructure (or at least make some inferences about their likely properties) that give the best fit with measured data. The data will be broken up into clear sky and overcast cases to eliminate competing effects of clouds and aerosols.

Secondly, as the model has never previously been used in the Antarctic we will also use this study to see how well the model predicts irradiances in the Antarctic environment. While this study is not intended to be a validation of the radiative transfer model we chose to use, the nature of the study lends itself to comparing modeled values of irradiance to measured values. The results of the comparison between modeled and measured irradiances will be discussed.

Next we will use the radiative transfer model to calculate the surface upwelling longwave and shortwave irradiances. A comparison will be made with the measured and modeled surface downward irradiances. Using the upward surface irradiances we will calculate a net irradiance and discuss its significance.

Finally, we will compare the model output to the results of empirical equations that predict downward shortwave and longwave surface irradiances. The equations were developed specifically as best fit predictors of the ANZFLUX data. Of interest is whether the model gives any added value over the empirical equations for predicting downward irradiance.

A short discussion of the vertical heat exchange equations will be followed by a description of the data used for the study, a description of the basics of the radiative transfer model used, methodology, the results of the study and a short summary.

II. VERTICAL HEAT EXCHANGE THROUGH THE ICE

The equation governing vertical heat exchange at the upper ice surface is shown below (Gow and Tucker, 1991).

$$(1 - \alpha)\, S_0 + I_0 + L_i + L_e + T_s + T_l + C_u - M = 0 \qquad (1)$$

Where α is the surface albedo, S_0 is the incoming solar radiation, I_0 is the shortwave flux that penetrates the ice, L_i is the incoming longwave radiation, L_e is the emitted longwave radiation from the upper surface, T_s is the sensible heat flux, T_l is the latent heat flux, C_u is the heat conducted through the boundary and M is the heat loss due to melting of the ice. Both radiative and turbulent processes contribute to the surface heat flux. However, T_s and T_l are small compared to the radiation terms, especially during the winter. Therefore the longwave surface radiation balance largely controls the surface heat budget of the Weddell Sea in the winter (Guest, 1996).

The equation for the vertical heat exchange through the underside of the ice is shown below.

$$Q_f + C_l + F_w = 0 \qquad (2)$$

Where Q_f is the heat loss or gain due to melting or freezing of the underside of the ice, C_l is the heat gain due to

conduction of heat from bottom of ice upward and F_w is the turbulent flux of heat from the ocean to the ice.

We will not be concerned with the heat budget of the lower ice surface except to realize that the ocean is the main source of heat during the winter months. The upper surface of the ice is colder than the interior during the winter months so heat is conducted upwards through the ice. During the summer months the main source of heat is incoming solar radiation.

III. DATA

The data used for this study was obtained during the 1994 Antarctic zone flux experiment, or ANZFLUX, conducted on the Weddell Sea ice pack during the austral winter (McPhee *et al.*, 1996). Two data sets were used, a longwave and shortwave downward surface irradiance record taken over the Weddell Sea ice pack and balloon-launched rawinsonde profiles of the atmosphere above the ice pack.

The data was collected from Julian day 195 (July 14), 1994 to Julian day 229 (August 17) onboard the *RV Nathaniel B. Palmer*. The track of the *RV Nathaniel B. Palmer* through the Weddell Sea ice pack is shown in Figure 1 with corresponding Julian days. Drift 1 and drift 2 on Figure 1 refer to periods of the cruise when ice camps were established on the ice pack and instruments were set up on the ice to collect data.

Permanently mounted sensors aboard the *RV Nathaniel B. Palmer* were used to continuously measure downward and upward longwave and shortwave irradiances while the ship transited the Weddell Sea ice pack during the Antarctic winter. A prygeometer was used to measure the downward longwave irradiance and a pyranometer was used to measure the downward shortwave irradiance. The prygeometer and pyranometer were

mounted on gimbals on an unobscured part of the ship so that they would point upward even when the ship rolled and pitched. The sensors were equipped with aspirators to prevent ice and frost buildup. The irradiance measurements were digitally recorded along with the time of measurement. Upward irradiance was measured using hand-held infrared sensors. The error of the downward shortwave and longwave irradiance measurements obtained by the two instruments was estimated to be about 4 Wm^{-2} for the shortwave and 6 Wm^{-2} for the longwave irradiances (Guest, 1996).

Eighty balloon-launched rawinsondes were used to digitally record atmospheric profiles of temperature, humidity, pressure, wind velocity and wind direction with respect to height. The rawinsondes were launched from the ship deck or ice surface at least twice every day. The rawinsondes were electronically tied into the ship's navigation system so that each rawinsonde recorded the time and position of launch. During the launches observers recorded the sky cover, unusual atmospheric content (such as diamond dust) and cloud bottom height. If the balloon looked as if it were going to pass through a cloud layer an observer would record the pressure at which the balloon disappeared into the clouds. This allowed for a reasonably accurate cloud bottom height determination estimated by Guest (1996) to be

plus or minus 20 m. If the cloud deck could be illuminated by surface lighting, then this method could be used at night. The amount of cloud cover could be determined at night as well since star obscuration gave a reasonable estimate of how much cloud cover existed.

Of the eighty soundings that were taken over the length of the cruise, many had defective profiles. If the defective segments were deleted, the data could still be used. If too much of the profile was missing or defective, the sounding was deemed to be unreliable and discarded.

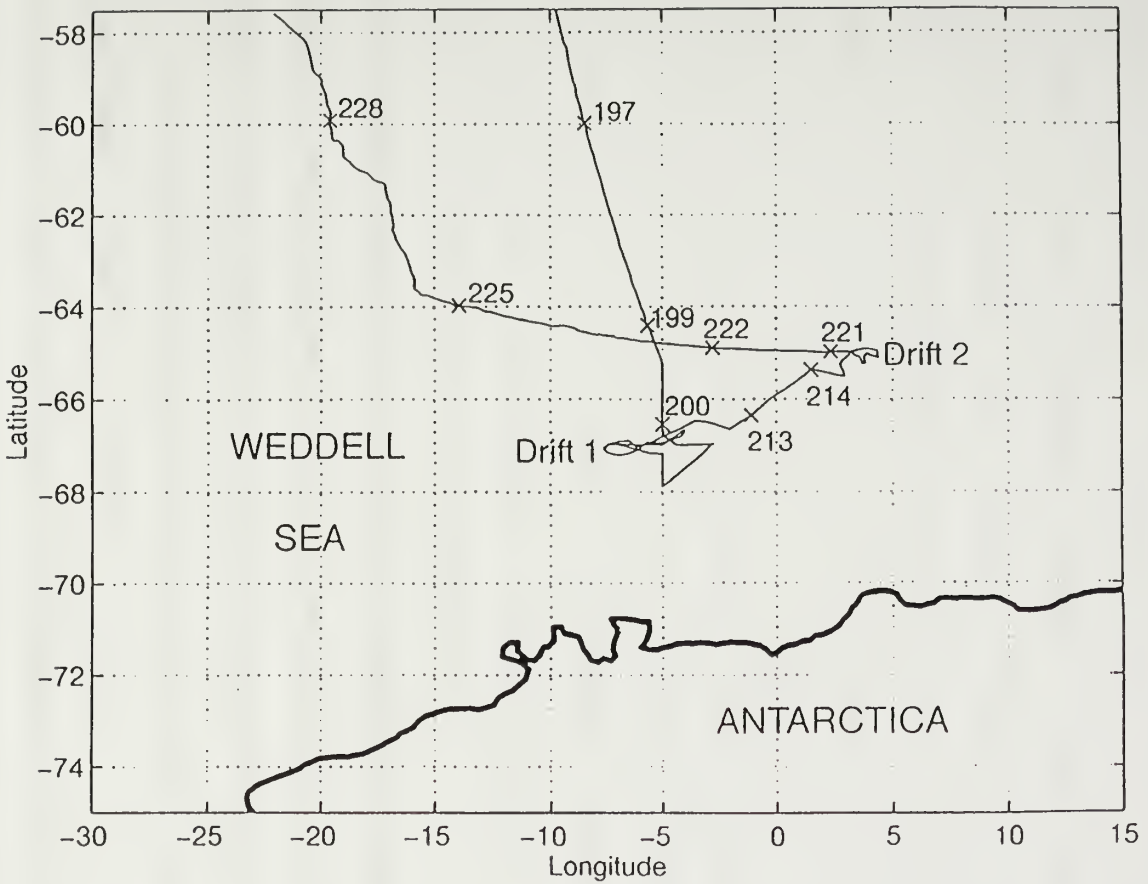

Figure 1. Track of RV Nathaniel B. Palmer from 14 July 1994 (Julian day 195) to 17 August 1994 (Julian day 229). Drift 1 and 2 indicate periods when ice camps were established.

IV. RADIATIVE TRANSFER AND MODEL DESCRIPTION

The model used to calculate radiative fluxes (irradiances) for this thesis is called STREAMER. STREAMER is a radiative transfer model that numerically solves the radiative transfer equation shown below based upon user input.

$$L_t(\lambda,\theta,\varphi) = L_0(\lambda,\theta,\varphi)e^{-\delta(\lambda)/\mu} + \int_0^{\delta(\lambda)}[\sigma_a(\lambda,z)B(\lambda,T(z))/\sigma_e(\lambda,z)]e^{-\delta(z,\lambda)/\mu}d\delta/\mu +$$

$$\int_0^{\delta(\lambda)}[\int_{4\pi}[\gamma_s(\theta,\varphi;\theta',\varphi';\lambda,z)L(\theta',\varphi';\lambda,z)/\sigma_e(\lambda,z)]d\Omega']e^{-\delta(z,\lambda)/\mu}d\delta/\mu \qquad (3)$$

STREAMER can compute intensities (radiances) or density fluxes (irradiances) for many different surface and atmospheric conditions (Key, 1996). The utility of STREAMER is that the model can be used to determine various atmospheric parameters as well as surface and atmospheric fluxes. STREAMER was developed by J. Key and A. Schweiger (Key, 1996) using gas absorption data and code from a program called *Strats* (Tsay *et al.*,1989), a discrete ordinate solver described in Stamnes et al. (1988), ice cloud optical physics from Ebert and Curry (1992), a two stream radiative transfer solution method from Toon et al. (1989) and water cloud optical physics from Hu and Stamnes (1993).

The major features (Key, 1996) of STREAMER include: 1) Fluxes (irradiances) may be computed using two or more streams, either broadband or narrow band. 2) Upwelling and

downwelling, shortwave, longwave, and net fluxes, cloud radiative effects, and heating rates can be computed. STREAMER uses 5 μm as the cutoff between longwave and shortwave radiation. Radiation of less then 5 μm is assumed to be of solar origin and is labeled shortwave. Radiation greater than 5 micrometers is assumed to be thermally emitted and of terrestrial origin and is labeled longwave. The electromagnetic spectrum broken down by wavelength is shown in Figure 2. 3) Gas absorption with overlapping gases and clouds are parameterized for 24 shortwave and 105 longwave bands, and gaseous absorption can be turned on or off. 4) Each computation is done for a particular scene, where the scene can be a mixture of up to 10 individual cloud types occurring individually, up to 10 overlapping cloud sets of up to 10 clouds each, and clear sky conditions. 5) Built in atmospheric data include water and ice cloud properties, five aerosol optical models, four aerosol vertical profiles, and seven standard atmospheric profiles. Either standard or user-defined profiles can be used, or total column amounts of water vapor, ozone, and/or aerosols can be specified. Standard profiles include tropical, mid-latitude, subArctic, and Arctic. 6) Various built-in surface types may occur within a scene with ocean and sea ice being the two used in this study. 7) The user interface provides for the ability to loop

up to ten variables at a time and for user customized output.

Data processing is set by user determined input options and by the input atmospheric profiles. More on this will be discussed in the chapter on methodology.

While the model worked very well for the purposes of this thesis, it has several limitations that should be mentioned. One is that the model does not include atmospheric refraction or spherical geometry. This means that shortwave downward fluxes for solar zenith angles greater than about 70 degrees are subject to error. The model will not compute shortwave fluxes when the solar zenith angle is greater than 90 degrees. This also means that while shortwave flux is routinely observed after the sun sets below the horizon, STREAMER will not account for it. In addition, only water vapor, oxygen, carbon dioxide, and ozone are considered for STREAMER's built in gaseous absorption model. While these gases are the major sources of absorption in the atmosphere, other gases also play a role. Key (1996) estimates that the exclusion of trace gases probably creates errors of only a few Wm^{-2} in the longwave fluxes.

STREAMER can be downloaded via anonymous ftp from stratus.bu.edu (ftp 128.197.75.84) or from the STREAMER homepage (both maintained by Boston University) at URL address

http://stratus.bu.edu/streamer/streamer.html. STREAMER is available in a UNIX and MSDOS version. An updated user's manual for STREAMER can be downloaded with installation and troubleshooting documentation. STREAMER and its user's manual are continually being revised, and the latest versions of both are available for download at the above ftp site or World Wide Web homepage.

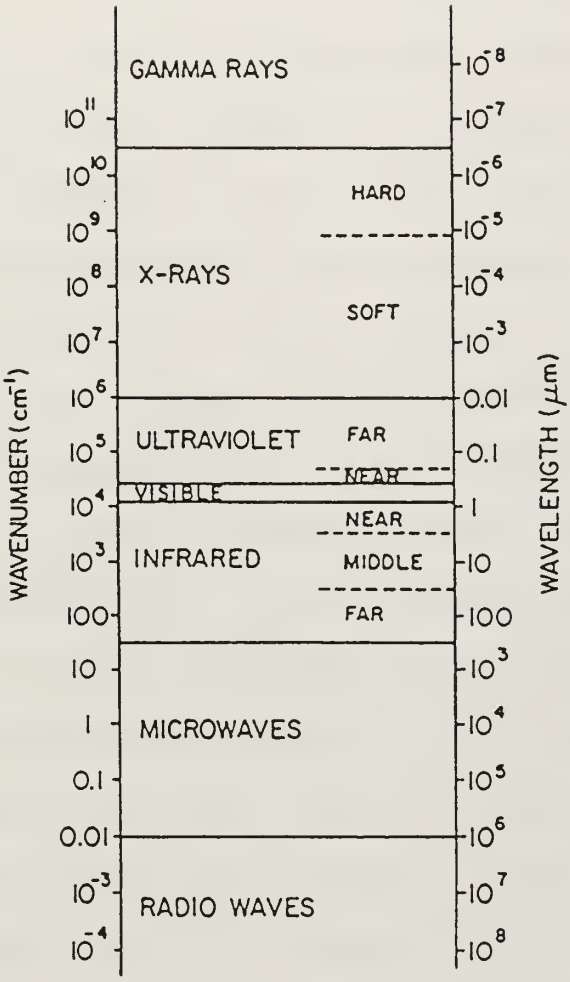

Figure 2. Electromagnetic Spectrum (from Kidder and Vonder Haar, 1995).

V. METHODOLOGY

A. DATA FORMATTING AND MODEL SETUP

To use STREAMER to solve the radiative transfer equation, formatted input files must be constructed. Examples of input files can be found in the STREAMER user's guide. These files are then read by STREAMER, and an output file is produced containing flux calculations for each particular case or scene input at any level/levels specified. Examples of output files can be found in the STREAMER user's guide. Most effort involved in using STREAMER is in building input files and in ensuring that the required input parameters are correct or logical. By building input files, varying input parameters and comparing the output of STREAMER with previously measured data deductions about the structure of the atmosphere above the Weddell Sea can be made. This structure affects the transfer of heat from the air-ice-ocean interface.

The first step to use the rawinsonde data in STREAMER was that it had to be formatted for insertion into STREAMER's input file. Of the nine variables measured by the rawinsonde only four are needed in the STREAMER input file. A MATLAB program was written which removed all of the header information of each rawinsonde data file. This data file was then processed by another MATLAB program which allowed needed

levels in the profile to be specified. This was necessary because while each of the soundings might contain hundreds of levels, STREAMER can process a maximum of 100 levels. In addition, the ability to scan the profiles and select desired levels was important because then low level temperature inversions present in some of the profiles could be included. This also allowed for quality control of the data and selectively screening out data that was bad or interpolating values for missing levels. The MATLAB program plots both the temperature and dewpoint versus height on the monitor, and then using the cursor the levels desired were marked. The program then automatically selects the height, pressure, temperature and relative humidity at the levels specified and writes this data to an output file. The monitor display is shown in Figure 3. Since STREAMER requires ozone concentration and aerosol extinction coefficients, profiles that were not measured by the rawinsonde, the program automatically sets these values to 0.0. The model used a standard assumed ozone profile for calculating absorption due to ozone. The program next plots temperature and dewpoint versus pressure (vice height in meters) on the monitor. Using the cursor, desired levels could be selected. The program then takes the selected levels and automatically outputs the corresponding pressure and temperature for the selected levels. This is used as a

method to determine location of cloud bases and tops and what their corresponding temperatures are in cases where clouds were present. This is shown in Figure 4. This data is also written to the same output file as the above height, pressure, temperature and relative humidity information. This information is then easily copied into the STREAMER input file. As mentioned earlier, STREAMER can only handle a maximum of 100 levels. If less than 100 levels are present STREAMER can automatically build the profiles from the top height input to 100 km using predefined standard atmosphere profiles based on work by Ellingson (1991) and Arctic Ocean coastal and drifting station data (Key, 1996). Since a profile was not available for the Antarctic winter, an Arctic winter profile was assumed to extend the soundings to 100 km.

With the data from the rawinsondes now formatted into the STREAMER input file, the work of assigning all of the remaining variables proceeded. STREAMER has several built in surface types used to model surface albedos. Since the area of interest was the Weddell sea ice pack, the surface types for the model were assigned as 95% snow (representing the top surface of the ice pack) and 5% open ocean (representing the small percentage of open ocean leads present). In addition to surface albedo the model also allows the user to set the surface emissivity. This value indicates how closely a

surface approximates a black body and is used to calculate the longwave irradiance emitted by the surface. The value used in the model was 0.95 for the ice/snow surface of the pack ice (Stull, 1988).

Unfortunately the model does not presently have the capability to handle multiple emissivity values if a variety of surfaces are being modeled. Therefore the emissivity used was the value for the largest percentage of surface area being modeled, the ice/snow surface. Latitude, longitude and time of the rawinsonde launch were taken directly from the original rawinsonde data files and put into the input file. This data was used by the model to calculate the sun's zenith angle so that the amount of incoming solar radiation could be determined. The model can be configured to calculate irradiances in the shortwave, longwave, or any of 129 different bands representing the spectral range. The model was configured to calculate irradiances for the entire spectrum.

B. CLEAR SKY CASES VERSUS OVERCAST CASES

Having assigned the variables that could easily be determined from the time, position and geography of the data set two factors were still unknown. These were aerosol content and distribution and cloud droplet size and water concentration. While the effects of clouds and aerosols in

the radiative transfer equation are understood the model was used to attempt to find the characteristics of these variables in the Weddell Sea environment. It was expected that the aerosols would play a very minor role in determining the longwave irradiances as their effect on longwave radiation is negligible (Kidder and Vonder Haar, 1995). The greatest effect of aerosols would be on shortwave irradiance. In order to determine the nature of aerosols and cloud microstructure the data was divided into two sets, clear sky cases and overcast cases. This was done to attempt to eliminate any competing effects of aerosols and clouds. Once a determination of aerosol type and distribution was made then this would be used in the overcast cases and properties of the cloud microstructure would be determined.

C. ERROR ANALYSIS

In order to make comparisons between the modeled and measured data, the average error, scatter error and total error were calculated. Average error, scatter error and total error refer to the mean, the standard deviation about the mean and the root mean squared (rms) of modeled irradiance minus measured irradiances. The equations for average error, scatter error and total error are shown below where Mod_i is the modeled data and $Meas_i$ is the measured data.

$$\frac{1}{N}\sum_{i=1}^{N}(Mod_i - Meas_i) = Average\ Err. \quad (4)$$

$$\sqrt{\frac{1}{N}\sum_{i=1}^{N}(Mod_i - Meas_i - (\frac{1}{N}\sum_{i=1}^{N}(Mod_i - Meas_i)))^2} = Scatter\ Err. \quad (5)$$

$$\sqrt{Average\ Err.^2 + Scatter\ Err.^2} = Total\ Err \quad (6)$$

In addition, a correlation coefficient was calculated to determine how well the modeled irradiances could be used to predict the measured irradiances. These statistics allowed us to determine which aerosol models, aerosol optical depths and cloud structure parameters resulted in the closest agreement between modeled and measured data.

D. CALCULATION OF TURBULENT FLUXES

To verify that turbulent heat flux was small in comparison to the radiant fluxes, both the sensible heat flux and latent heat flux were calculated. The turbulent fluxes, sensible and latent are represented by the following equations

$$T_s = \rho_a C_p C_{HN} U_{10} (T_a - T_{sfc}) \quad (7)$$

$$T_l = \rho_a L_v C_{QN} U_{10} (q_a - q_{sfc}) \quad (8)$$

where ρ_a is the density of air, U_{10} is the wind speed at 10 m, C_p is specific heat, L_v is the latent heat of evaporation, the sensible and latent heat transfer coefficients C_{HN}, C_{QN} fall within the range $1.0 \times 10^{-3} \leq C_{HN}, C_{QN} \leq 1.5 \times 10^{-3}$ (Andreas,

1987), T_a and T_{sfc} are the temperature at 10 m and the surface temperature and q_a and q_{sfc} are the specific humidities at 10 m and at the surface.

The data set used did not measure specific humidity and so it was calculated using the measured temperatures , pressures and relative humidities. This was done using the following method. First, the saturation pressures of water vapor over water at the surface and at 10 m were calculated using equation 9.

$$e_s(T) = 6.112e^{\frac{17.67T}{T+243.5}} \qquad (9)$$

Next, the saturation pressures of water vapor over ice at the surface and at 10 m were calculated using equation 10

$$e_i(T) = \frac{e_s(T)}{(\frac{273}{T})^{2.66}} \qquad (10)$$

where T is the temperature at the desired level. Then the partial pressure of water vapor e was calculated over water and ice using equations 11 and 12

$$e = e_s \; x \; R.H. \qquad (11)$$

$$e = e_i \; x \; R.H. \qquad (12)$$

where R.H. is the relative humidity at the desired level.

Finally, the specific humidity was calculated using 13

$$q = .622 \frac{e}{p - (1 - .622)e} \qquad (13)$$

where p is the pressure at the desired level.

Because it was estimated that the surface being considered was 95% ice and 5% open water lead, sensible heat fluxes and latent heat fluxes for both water and ice were calculated for each case. The heat fluxes over ice were multiplied by 0.95, the heat fluxes over water were multiplied by 0.05 and the two added together to get an areal average heat flux contribution for sensible and latent heat. The calculated values are discussed in the chapter on results.

E. DETERMINATION OF AEROSOL STRUCTURE

STREAMER models the effects of aerosols by using extinction coefficients (km^{-1}) at each designated atmospheric level. This extinction coefficient, σ_e, is a combination of both absorption, σ_a, and scattering, σ_s, effects at each wavelength. This is represented by the following equation.

$$\sigma_e(\lambda, z) = \sigma_a(\lambda, z) + \sigma_s(\lambda, z) \qquad (14)$$

The extinction coefficient times the thickness of the layer gives the optical depth, δ, of the layer. The sum of the optical depths for each layer gives the total optical depth of the atmosphere as shown in the following equation.

$$\delta(z,\lambda) = \int_{sfc}^{z} \sigma_e(\lambda, z)\, dz \quad (15)$$

The extinction coefficients can be assigned to each level either by a user-supplied profile or by a model-supplied profile. If an extinction coefficient profile is not assigned (in this case the extinction coefficients were not measured), then either an aerosol model or a column optical depth can be specified.

Our approach was to solve the model using the clear sky cases with different aerosol profiles supplied by the model and with different values of total column optical depth. By taking the modeled downward shortwave and longwave irradiances and comparing them to the measured downward longwave and shortwave irradiances an attempt was made to deduct which aerosol model or optical depth was the most realistic. As mentioned above, it was expected that aerosols would not greatly affect the longwave irradiances. Due to the relatively short time the sun was above the horizon each day there was a lack of soundings taken during the daylight. Most of the measured and calculated shortwave irradiances were zero.

Model solutions were obtained with an Arctic aerosol model, a marine aerosol model and total column optical depths ranging from 0.0 to 0.08. This range of optical depth was selected based upon the work of Weller and Leiter (1988). An

error analysis was conducted comparing the modeled to the measured data.

The marine aerosol optical model gave the best results and this model was used for the rest of the irradiance calculations. This result will be discussed in more detail in the chapter on results.

F. DETERMINATION OF CLOUD MICROSTRUCTURE

The next step was to examine the overcast soundings. The criteria for overcast was 100 percent cloud cover. Thus the percentage of cloud cover in the model was set at 100 percent. As the effects of cloud cover in the radiative transfer equation are understood, it was hoped to use the model to identify some of the microstructure of cloud cover that influences the longwave and shortwave radiation budget of the Weddell Sea. While there is a fair amount of information on cloud microstructure in the mid-latitudes, information on Antarctic cloud microstructure is quite sparse (Feigelson, 1984). The primary interest was to use the model to get an idea of what droplet effective radii, cloud water concentration and droplet type (liquid or ice) gave the closest representation of the cloud structure over the Weddell Sea. The hope was that selecting these parameters correctly would result in modeled irradiance calculations that were the closest to the actual measured irradiances. To do this, all of

the overcast rawinsonde soundings were modeled. These soundings are shown in Table 1. While processing these soundings for inclusion into the STREAMER input files, some were identified where it was too difficult to make a reasonable estimate of where the cloud tops were based upon the sounding profiles. These soundings are indicated with an asterisk or double asterisk in Table 1.

Another problem which was identified while processing these soundings was whether to model the droplets in each sounding as water droplets or ice crystals. It was decided to use a -20^0 C cutoff for ice crystal formation (Rogers and Yau, 1989). If the temperature in the identified cloud layer were colder than -20^0 C, then the model would be applied once with the droplet treated as an ice crystal and again with it treated as a water droplet. For those soundings where the identified cloud layer was warmer than -20^0 C the model was run only with the droplet treated as a liquid droplet. The soundings where the droplets were treated as both liquid and ice are indicated in Table 1. In addition, Table 1 shows the cloud bottom pressures and temperatures, cloud bottom height in meters and the cloud thickness measured in millibars. The model unfortunately assumes a homogeneous cloud microstructure and allows for only one choice of droplet type, droplet radius and water concentration.

Snd#	Julian Day	Cloud Base	Cloud Top	Thick. (mb)	Bott. Press.	Bott. Temp.	Rel. Humid.	Ice Cloud?
11	196.41	380 m	720 m	39	921 mb	-5.0	85	No
12	196.53	291 m	1050 m	88	929 mb	-3.7	88	No
15	197.43	474 m	1100 m	73	915 mb	-11.2	90	No
30	205.52	291 m	480 m	83	935 mb	-13.8	83	No
32	206.53	300 m	430 m	17	945 mb	-19.2	88	Maybe
30	206.95	318 m	420 m	14	953 mb	-22.1	88	Maybe
30	207.52	305 m	420 m	15	955 mb	-22.4	81	Maybe
36	208.47	170 m	900 m	88	951 mb	-13.8	78	No
39*	210.45	365 m	????	9 ??	935 mb	-23.1	75	Maybe
41	211.46	531 m	690 m	16.6	918 mb	-21.9	93	Maybe
43	212.45	365 m	480 m	14	942 mb	-14.9	85	No
45	213.44	270 m	530 m	32	935 mb	-15.6	90	No
47*#	214.44	5128 m	????	126.8?	471 mb	-43.5	93	No
58	216.47	200 m	480 m	34.9	956 mb	-10.7	93	No
54	217.46	797 m	1320 m	59.8	863 mb	-21.7	93	Maybe
55*	218.46	623 m	????	23 ??	935 mb	-10.6	78	No
58	219.54	380 m	480 m	52.5	926 mb	-10.6	84	No
62	221.52	639 m	760 m	14.5	896 mb	-22.7	71	Maybe
71	225.46	298 m	690 m	47	951 mb	-8.5	88	No
76	228.00	185 m	530 m	41.9	966 mb	-6.1	91	No
77**	228.45	160 m	400 m	29.5	966 mb	-10.7	88	No
78	228.71	183 m	810 m	74	965 mb	-7.2	82	No
	* Sounding too ambiguous to make guess of cloud top							
		# Mid-level cloud deck						
	** Due to equipment problems, no measured fluxes							
		-20 C used as cutoff for ice clouds						

Table 1. Overcast soundings cloud information.

While it is difficult to measure cloud macroscopic properties such as height, thickness and temperature, it is even more

difficult to measure cloud microstructure such as cloud droplet number, droplet radius and type. Using the model the dominant microstructure affecting longwave and shortwave radiation could be deducted, but in reality clouds are often a nonhomogeneous mixture of these variables (Paltridge and Platt, 1976). The range of values used for water droplet effective radius was 2.5 to 60 microns, which brackets most of the natural variability found on earth (Wiscombe, 1977). The liquid water concentration range for clouds was set between 0.05 gm^{-3} to 0.5 gm^{-3} (Feigelson, 1984). Ice crystal effective radius ranged between 13 microns and 130 microns (Paltridge and Platt, 1976). Ice water concentration in the clouds was taken to range from 0.0002 gm^{-3} to 0.07 gm^{-3} (Liou, 1992). Since it was necessary to be able to see when the rawinsonde disappeared into the cloud bottom to get a measure of the cloud base height, there were a lot of cases where shortwave irradiance calculations gave a non-zero value. As in the aerosol determination, the model was solved with the soundings listed in Table 1 using the above listed ranges of values. After the model solutions were completed, the data was compared with the measured longwave and shortwave irradiances. An error analysis was performed on the output and a correlation coefficient, average error, scatter error and total error calculated.

Of interest was whether the model could provide a more precise value of the drop effective radii and water concentrations that gave the best agreement with the measured downward longwave and shortwave irradiances for each case. To determine what values of drop effective radii and total cloud water concentration best represented the actual cloud for the shortwave and longwave cases, more model solutions were conducted. It was decided to use the results of the error analysis to decide how to vary the droplet radii and cloud water concentration. Since in the longwave case the best results were obtained by using an effective radius of 2.5 microns, the cloudy cases were again solved holding the effective radius constant and varying the water concentration. For the shortwave case, since the best results seemed to be obtained at the end values of the allowed ranges, the model was solved again with the values of droplet effective radius and water concentration varying from 2.5 microns and 0.05 gm^{-3} to 60 microns and 0.5 gm^{-3} linearly. The data was then analyzed to see which combination of effective radius and water concentration gave the value closest to the measured downward longwave and shortwave irradiances. In general, the best fit in both the longwave and shortwave is achieved by clouds that have smaller droplets and a low water concentration. The results of this analysis will be discussed

in more detail in the chapter on results.

G. CALCULATION OF UPWELLING SURFACE IRRADIANCES

Next, STREAMER was used to calculate the upwelling longwave and shortwave surface irradiances. Using the best fit aerosol model and cloud microstructure parameters established above, the model was run again using the clear sky and overcast sky cases. In this way it was attempted to set up the model as realistically as possible for the physical environment present during the ANZFLUX soundings. An error analysis was conducted by comparing the modeled upward surface irradiances with the measured upward surface irradiances. A discussion of the modeled upward surface irradiances follows in the results chapter.

H. CALCULATION OF EMPIRICALLY DERIVED DOWNWARD SURFACE IRRADIANCES

A comparison of the modeled longwave and shortwave downward irradiances was made with empirical equations developed by Guest (1996) during his work in the ANZFLUX project. These empirical formulas were developed to predict downward shortwave and longwave irradiance for the cases of a completely clear sky and a completely overcast sky. Of interest was whether of not these simple empirical relations were more accurate than a model which attempted to represent the physics of radiative transfer. The empirical formulas used are shown below.

$$SW\downarrow(clear) = S_0(12.46 \times 10^{-3} + 0.336\cos(Z) + 1.43\cos(Z)^2) \quad (16)$$

$$LW\downarrow(clear) = \sigma T_{air}^4 - 85.6 \quad (17)$$

$$SW\downarrow(overcast) = S_0(6.43\times10^{-3}+0.182\cos(Z)+0.826\cos(Z)^2) \quad (18)$$

$$LW\downarrow(overcast) = \sigma T_{air}^4 - 18.7 \quad (19)$$

Z is the zenith angle with 90 degrees taken to be the horizon. S_0 is taken to be 1367 Wm^{-2} (Garratt, 1992). T_{air} is the air temperature measured from the ship's deck. The equations were developed not to model the physics of radiative transfer but were developed specifically as a best fit solution to the ANZFLUX data set (Guest, 1996). For these equations the shortwave irradiances for both the clear and overcast cases are taken to be zero for a zenith angle greater than 90 degrees, i.e., when the sun is below the horizon. As will be discussed in the results chapter, this is not a very realistic assumption.

The modeled data using STREAMER with the aerosol and cloud characteristics determined above was compared against irradiances produced by the empirical equations. This was done by comparing the error analysis done above on the modeled STREAMER data with an error analysis conducted on the measured and empirically derived data. While it would have been possible to use different values of drop effective radius and

water concentration in the model for each specific case in order to greatly reduce error, it was decided to use the overall best fit values of these parameters (2.5 microns and 0.05 gm^{-3}) in all of the cases and compare the model solutions as a whole against the empirical relationships.

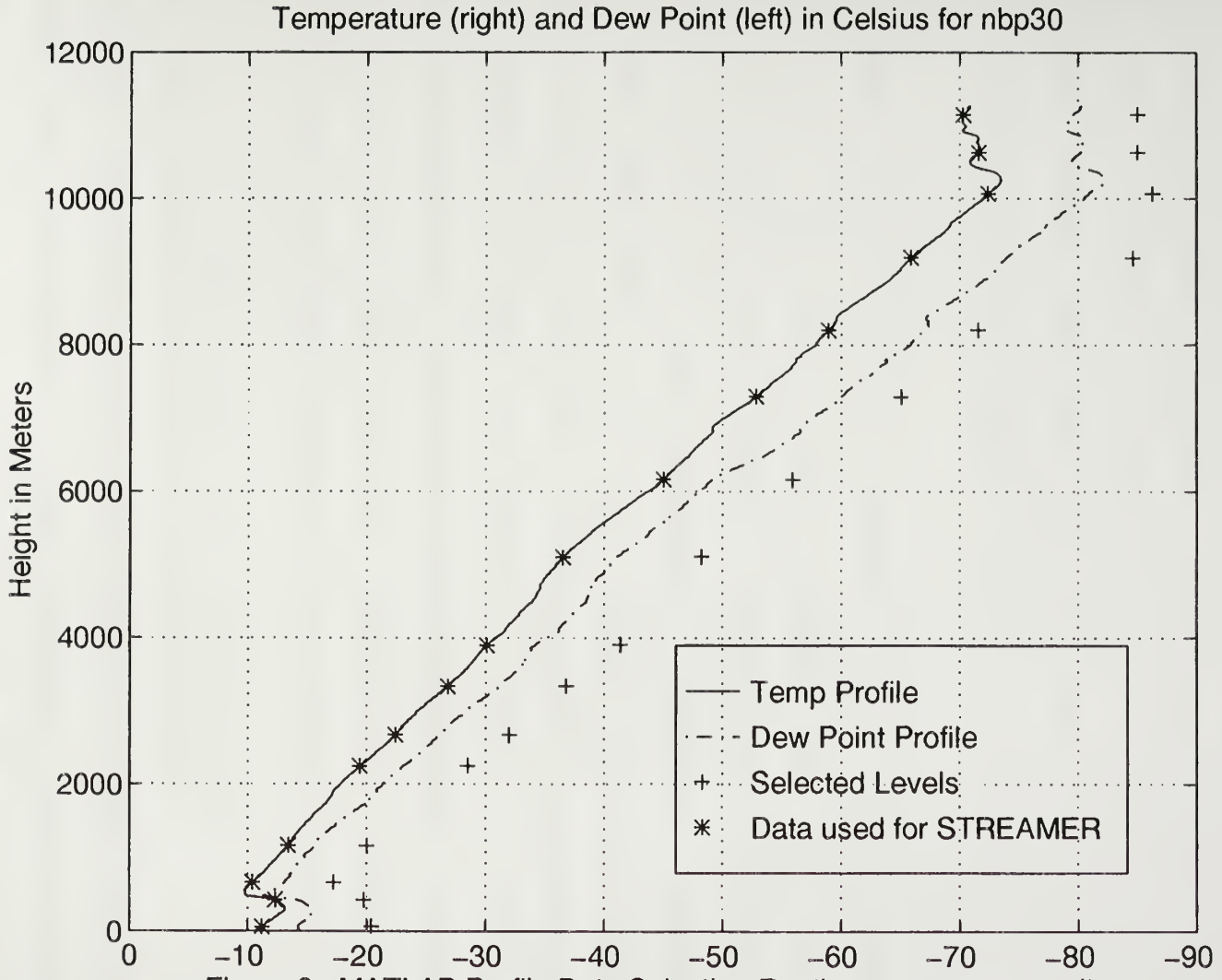

Figure 3. MATLAB Profile Data Selection Routine as seen on monitor.

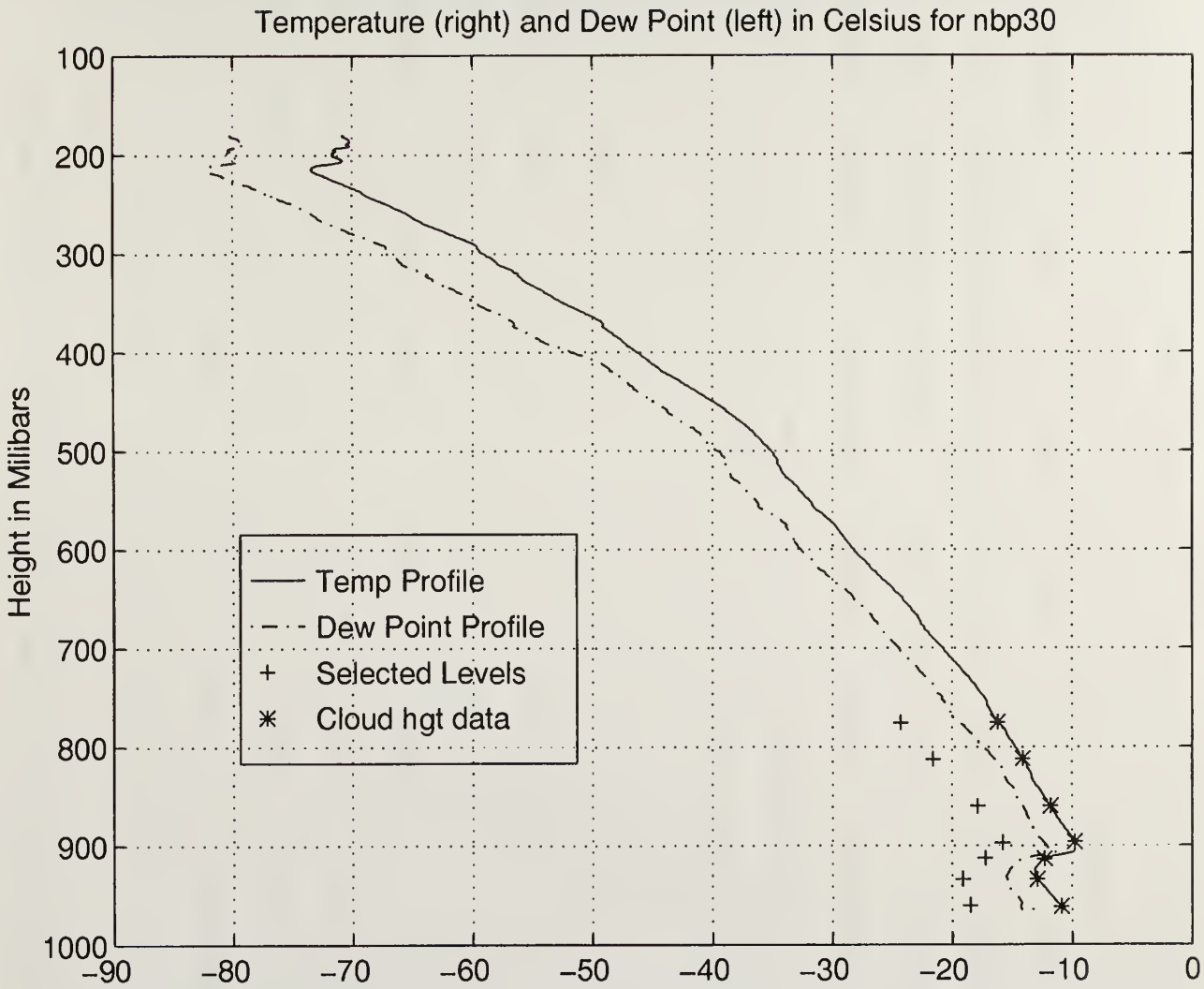

Figure 4. MATLAB Cloud Top and Base Selection Routine as seen on monitor.

VI. RESULTS

A. DISCUSSION OF TURBULENT HEAT EXCHANGE

The turbulent heat fluxes were calculated for all of the cases and the results are shown in Figure 5. Average values are shown by solid lines. The average sensible heat flux was 33.3 Wm^{-2} directed upward and the average latent heat flux was 4.5 Wm^{-2} directed upward. Note that these are arealy-averaged values that take into account the small percentage of area that exists as open water leads. As expected, the latent heat contribution was minimal, but the sensible heat term was significant. The majority of the sensible heat flux is from the open ocean leads since the ocean is so much warmer than the air above it. This heat can then be advected out over the ice surface and cause warming which results in increased longwave radiation upward. Exactly how sensible heat from open water leads flows is an important factor in the surface heat budget. If this heat can escape upward without being advected over the ice, it will not affect the surface heat budget as much as when it is advected horizontally over the ice fields.

B. DETERMINATION OF AEROSOL STRUCTURE AND AEROSOL EFFECTS

The effects of aerosols, dust, salts, dimethyl sulfides and snow crystals in the scattering of radiation is a function

of viewing geometry, particle shape, size and index of refraction and radiation wavelength. The size parameter equation shown below, where λ is the incident radiation wavelength, r is the particle radius and χ is the size parameter, can be used to relate the scattering of radiation to the size of the particle and the incident radiation's wave length.

$$\chi = \frac{2\pi r}{\lambda} \qquad (20)$$

This equation can be used to divide scattering into three types according to the size of the particle and the wavelength of the incident radiation. This is illustrated in Figure 6 (Kidder and Vonder Haar, 1995). The shortwave irradiance, because of its size parameter, falls into the Mie scattering regime while the longwave irradiance falls mostly into the Rayleigh scattering regime. Its effects are expected to be negligible because scattering in the Rayleigh regime has a χ^4 dependence and the size parameter χ for longwave radiation interacting with aerosols is small. Therefore it was expected that most of the scattering effects of aerosols would be in the shortwave regime, and that is what was observed.

The determination of aerosol effects and structure was difficult and possibly ambiguous for two reason. First, data was lacking in the clear sky cases where the sun was above

the horizon. Therefore, for most of the clear sky cases both the modeled and the measured shortwave (solar) radiation were zero. Second, because of the extremely low zenith angle of the sun in the Antarctic during the austral winter, the shortwave irradiances predicted by STREAMER are subject to error. This is because the model does not include atmospheric refraction or spherical geometry, important for solar zenith angle greater than 70 degrees. In this study all of the soundings had solar zenith angles greater than 80 degrees. In addition, the model always predicts that shortwave irradiance will be zero when the sun is below the horizon. From common experience it is recognized that even when the sun is below the horizon some visible radiation still exists due to refraction.

Despite these weaknesses it was decided to still apply the model to the clear sky cases to learn about aerosol effects and structure and to compare the model predictions with observations. Since aerosol content was not measured, model solutions were calculated over a series of different optical depths starting from completely aerosol free (optical depth 0.0) to the maximum optical depth that seemed, based on prior research, to be physically reasonable (optical depth 0.08). This upper bound was based upon the work of Weller and Leiterer (1988). Model solutions using some of the built in

aerosol models supplied, a marine aerosol model and an Arctic aerosol model, were calculated.

The air in Antarctica is some of the cleanest in the world and so the starting point was a completely aerosol free atmosphere. The air in the Arctic, while still relatively clean, has a large amount of anthropogenic aerosols from the industrial activities of eastern Europe. Thus for comparison purposes the model was also solved with the Arctic aerosol model. The results of the error analysis are shown in Table 2.

The first and most obvious effect was that aerosols do not seem to have any major effect on longwave radiation, at least at the aerosol optical depths used. For the different aerosol models and optical depths solved, the effect on longwave downward irradiance was less than 0.7 Wm^{-2}. This was expected because of the large wavelength in relation to aerosol size discussed earlier. This is not to say that aerosol content is unimportant to the overall heat budget of the air-ice-ocean interface in the Weddell sea. During the austral winter while the amount of direct solar heating is relatively small due to large solar zenith angle and minimum amount of time of solar exposure, the majority of heat flux comes from the warming due to the ocean underneath the ice.

Optical Depth	0.0	0.001	0.01	0.08	Marine Aer. Mod	Arctic Aer. Mod
		Correlation Coefficient				
swd	.9493	.9493	.9497	.9510	.9536	.9517
lwd	.9516	.9514	.9502	.9363	.9525	.9384
		Average Error (W/m^2)				
swd	9.026	8.922	8.048	2.852	1.566	2.774
lwd	-2.653	-2.6	-2.104	1.563	-2.023	1.865
		Scatter Error (W/m^2)				
swd	17.25	17.2	16.72	14.32	13.6	14.2
lwd	5.533	5.54	5.601	6.283	5.487	6.186
		Total Error (W/m^2)				
swd	19.47	19.37	18.55	14.6	13.69	14.47
lwd	6.136	6.12	5.983	6.475	5.848	6.461

Table 2. Aerosol Error Analysis.

During the austral summer, aerosol effects become much more important as the relative effect of solar radiation becomes more important in the direct heating of surfaces and the subsequent reemitting of thermal radiation. The main point is that for the austral winter the dominant irradiance is in the longwave and this is not significantly affected by aerosols.

The second effect noted was that increasing the amount of aerosols (by increasing the magnitude of optical depth in the model) resulted in decreasing levels of downward shortwave irradiance. This was expected, as placing more optically active material in the path of the downward solar irradiance

should result in more of it being scattered. For example, increasing the optical depth from 0.0 to 0.08 in STREAMER resulted in an average decrease of model predicted solar irradiance of 5.0 Wm^{-2}.

The structure of the aerosol content in the Antarctic atmosphere was best modeled by using the maritime aerosol optical model. While this model resulted in the lowest magnitude of error as seen in Table 2, it was by no means decisively superior to either a total column optical depth of 0.08 or to the arctic aerosol model. The extinction coefficient versus wavelength profile of the maritime aerosol optical model is shown in Figure 7 (Key, 1996). Note that as discussed above, the extinction coefficients become negligible as the wavelength increases. Both the marine and the arctic aerosol optical models used in STREAMER were run using an aerosol loading scheme in which the aerosols are present in background levels still allowing for at least 50 km visibility in the troposphere. The total optical depth of both the Arctic and marine models is set to 0.08. This seems very reasonable in light of the relatively clean air in the Antarctic. It appears that the Weddell Sea air is not optically transparent and resembles the aerosol structure of arctic air or of marine air that has an optical depth of 0.08. The use of a profile with varying extinction coefficients with

height seems to better describe what is happening in the Antarctic air than just using a total column optical depth of 0.08. As the Weddell Sea is influenced by major storm events in the winter, perhaps marine aerosols are advected into the region or are mixed into the atmosphere from existing leads in the pack ice. In addition, the possibility exists that the effect observed is not due to marine aerosols at all but aerosols made up of bits of snow and ice blown up into the atmosphere from the surface of the ice. The resemblance of the Weddell Sea aerosol structure to that of a maritime environment is not unexpected. Jaenicke (1993) has found that in the mixed layer, maritime and polar aerosol concentrations can behave similarly in that both share a similar concentration profile with height. The main difference is that as altitude increases, the maritime aerosols seem to reach a higher background concentration than polar aerosols. The optical depth of 0.08, while certainly not unreasonable, was slightly higher than expected from zonal averages.

However, recent work by McCormick *et al.* (1993) might present a possible explanation. Using the Stratospheric Aerosol Measurement II (SAM II) package on board the Nimbus 7 satellite to study stratospheric aerosols and clouds, they found distinctive jumps in optical depth in the stratosphere due to the recurrent formation of polar stratospheric clouds

(PSCs). These cloud types form in the Antarctic winter and then disappear in the Antarctic summer. These formation events lead to a significant optical depth enhancement in the austral winter and a decrease in the spring and summer. The higher optical depth that the model seems to indicate might be a result of PSC formation. In addition, Liou (1993) states that these clouds can also act to reduce the radiative cooling of the surface.

Unfortunately, due to the limited number of clear sky cases, it is difficult to determine the significance of the results. As shortwave output from STREAMER with solar zenith angles greater than 70 degrees is subject to error, these results might not reflect reality. More study with many more clear sky cases is needed to verify these results.

Since the marine aerosol optical model gave the smallest error, although by an extremely small margin, and since aerosol choice had such a negligible affect on longwave irradiance, it was decided to use this model in the rest of the runs involving overcast cases where the primary interest was at looking at the effects of clouds and cloud microstructure.

C. DETERMINATION OF CLOUD MICROSTRUCTURE AND CLOUD EFFECTS

Since cloud droplets are so much larger than air molecules and aerosols the size parameter χ increases for both

longwave and shortwave radiation. As illustrated in Figure 6, shortwave radiation now falls into the Geometric Optics scattering regime and longwave radiation falls into the Mie scattering regime for cloud droplets. In the Mie regime the wavelength of the radiation and the size of the droplet are comparable and so there is considerable interaction with the particle. In the Geometric scattering regime the cloud droplets scatter radiation by both reflecting radiation incident upon it and refracting radiation that comes near it.

Shortwave radiation interacting with cloud droplets has a relatively high scattering coefficient and therefore a relatively small mean free path (Kidder and Vonder Haar, 1995). This means that shortwave radiation entering a cloud does not have to travel very far between scattering events. Thus even a relatively thin cloud can scatter almost all of the incident radiation upon it. Liquid water is a poor absorber of shortwave radiation so almost all of the incident shortwave radiation on cloud droplets is scattered. While the scattering mechanics of ice crystals are more complex than that of spherical water droplets, they also scatter almost all of the incident shortwave radiation incident upon them (Liou, 1992). As the thickness of the cloud increases, the result is that more of the incident radiation is scattered out of the top of the cloud and less is scattered out of the bottom. The

end result of the interaction of downward shortwave radiation with clouds is that the amount reaching the surface, as compared to a clear sky case, will be reduced.

The longwave radiation interacts with the cloud droplets in the Mie scattering regime. While longwave radiation interacting with cloud droplets also has a relatively high scattering efficiency, the situation is changed by the fact that in the longwave spectrum water droplets absorb almost all of the radiation incident upon them. *Kirchhoff's law* states that a body is as good an emitter as it is an absorber. Thus clouds behave very nearly like blackbodies. Since water is a better absorber than ice, clouds consisting of ice crystals also behave like blackbodies but not as closely as clouds consisting of water droplets (Liou, 1992).

The soundings with overcast sky conditions that were used to examine effects of clouds and cloud microstructure are shown in Table 1. There was some ambiguity in determining cloud thickness for these cases. The cloud bottom was fairly accurately measured by observing the rawinsonde as it disappeared into the cloud base. The cloud top was estimated using the temperature dew point spreads as illustrated in Figure 4. There was some inaccuracy in estimating the cloud top height and therefore the cloud thickness using this method. It was expected that this would make the biggest

difference in the determination of downward shortwave irradiance and little difference in the calculation of downward longwave irradiance. This is because since clouds are such good absorbers and emitters, the downward longwave irradiance would depend on the temperature of the cloud base and relatively little on the cloud thickness. For the shortwave downward irradiance, however, cloud thickness would be a determining factor in how much radiation got through.

The clouds were all stratiform in nature and except for one sounding, low level. The exception was sounding 47, which had a much higher base and was considered to be a mid level cloud. It was not used, however, because its dewpoint and temperature profiles were too ambiguous to make a reasonable estimate of cloud top height.

To determine the most likely cloud drop or ice crystal size and water concentration the same technique as with the aerosol determination was used. Using realistic ranges outlined in the methodology chapter model solutions were calculated and the downward shortwave and longwave irradiances were compared with the measured values. The situation was complicated further by the fact that some clouds were cold enough that the presence of ice crystals was likely. These soundings are indicated in Table 1. Therefore the model was run with these clouds treated as both ice clouds and liquid

water clouds. A noted weakness of the model is that it allows for only one value of cloud drop or ice crystal effective radius and only one value of water concentration per cloud while in reality a distribution of droplet and or crystal sizes and water concentrations may exist in a single cloud. However, the model was used to attempt to find the particle size and water concentration which had the greatest effect on the incoming radiation. The first run that was conducted used the four extremes of possible droplet size and water concentration as a starting point. The modeled downward irradiances were compared to the measured values and an error analysis conducted. The results of the error analysis are summarized in Table 3. The modeled runs where some of the clouds were treated as consisting totally of ice crystals produced very large errors. In the shortwave, the ice crystals scattered too much radiation out of the bottom of the cloud and gave erroneously high values. In the longwave, the ice crystal clouds did not emit enough downward radiation and gave erroneously low values. Based on this, the clouds were treated as being composed of liquid water droplets for the rest of the study. This seemed reasonable since treating the clouds as water drops gave the best results overall and because it made sense that the low stratiform clouds would consist of liquid water droplets.

Eff. Radius Water Conc.	2.5 Microns .05 g/m^3	2.5 Microns .5 g/m^3	60 Microns .05 g/m^3	60 Microns .5 g/m^3
	Correlation Coefficient			
Liq. swd	.9605	.7749	.9062	.975
Liq./Ice swd	.7915	.5324	.914	.9302
Liq. Lwd	.9762	.981	.9624	.9604
Liq./Ice lwd	.9142	.9458	.9598	.9559
	Average Error (W/m^2)			
Liq. swd	-4.551	-25.88	10.38	2.269
Liq./Ice swd	3.554	-16.24	13.41	5.897
Liq. lwd	.2924	8.301	-64.08	62.49
Liq./Ice lwd	-20.2	.5474	-64.98	61.25
	Scatter Error (W/m^2)			
Liq. swd	5.627	14.27	21.33	6.864
Liq./Ice swd	20.87	21.32	22.71	12.8
Liq. lwd	6.852	4.747	6.63	6.863
Liq./Ice lwd	33.31	13.41	6.873	7.416
	Total Error (W/m^2)			
Liq. swd	7.237	29.55	23.72	7.229
Liq./Ice swd	21.17	26.8	26.16	14.09
Liq. lwd	6.858	9.563	64.42	62.86
Liq./Ice lwd	38.96	13.42	65.34	61.7

Table 3. Eff. Rad./Water Concentration Error Analysis.

The drop effective radius and cloud water concentration that gave the best modeled irradiances for the shortwave were not immediately clear. For an effective droplet radius of 2.5 microns and water concentrations of 0.05 gm^{-3} and an effective droplet radius of 60 microns and water concentration of 0.5

gm^{-3} the total error was very close.

For the longwave downward irradiance values, the best results were obtained for clouds with an effective radius and water concentration of 2.5 microns, 0.05 gm^{-3} and 2.5 microns, 0.5 gm^{-3}.

The next step was to make expanded model runs to see if the best fit drop effective radius and cloud water concentration could more closely be determined. Using the model output with varying drop effective radii and water content a data set was constructed of the best fit data with its corresponding drop radius and water concentration. These best fit drop radii and water concentrations are plotted on Figure 8. The majority of cases of best fit modeled data have smaller drop effective radii and low water concentrations. Note that some values plotted over each other so it is not entirely obvious how many values are plotted. To distinguish between longwave and shortwave data, they are plotted with different symbols. This plot shows that the best fit values of irradiances for the longwave have values of droplet effective radii and water concentration grouped toward the 2.5 micron and 0.05 gm^{-3} corner of the plot. The best fit shortwave irradiances have values of effective radii and water concentration grouped along a line extending from the 2.5 micron and 0.05 gm^{-3} corner of the plot to the 60 micron 0.5

gm^{-3} corner of the plot with most of the values occurring at the two ends. Since irradiances with the same droplet effective radius and water concentration plot over each other in this plot, histograms showing the amount of times best fit data had certain values of droplet effective radii or water concentration were plotted.

The longwave histogram (Figure 9) shows the number of times the best fit irradiance was produced for different water concentrations. In this case the drop effective radius was kept constant at 2.5 microns and just the water concentration was varied. For the shortwave case two histograms were produced, one showing the number of occurrences of a best fit with varying effective radius (Figure 10) and the other showing the number of occurrences of a best fit with varying water concentration (Figure 11). All of the best fit values of downward longwave irradiance had a drop effective radius of 2.5 microns and the majority of water concentration values between 0.05 gm^{-3} and 0.1 gm^{-3}. The best fit shortwave values had the majority of its radius values between 2.5 microns and 8.0 microns and the majority of water concentrations between 0.05 gm^{-3} and 0.1 gm^{-3}. The shortwave cases also had a fair number of values fall into the 60 micron and 0.5 gm^{-3} range. Since Table 3 shows that the total error between this and the 2.5 micron and 0.05 gm^{-3} values for the shortwave was almost

identical and that the error using 60 microns and 0.5 gm^{-3} was extremely large, it was decided that the cloud microstructure was best represented by a cloud droplet effective radius of 2.5 microns and a cloud water concentration of 0.05 gm^{-3}. This is certainly not unreasonable. Rogers and Yau (1989) state that the liquid water content of stratus clouds is usually in the range of 0.05 to 0.25 gm^{-3}. Liou (1992) shows droplet radius distributions for stratiform clouds at lower latitudes with modal peaks at 3.5 microns for oceanic stratus and 4.5 microns for continental stratus clouds. The study indicates that the Weddell Sea stratus is not too different in structure than stratus at lower latitudes.

Having determined a reasonable estimate of cloud drop effective radius and cloud water concentration, the modeled downward longwave and shortwave irradiances were plotted along with the measured downward irradiances as a function of Julian day for the clear sky cases, Figure 12, the overcast cases, Figure 13 and the both cases combined, Figure 14. This was done so that the effects of cloud cover on the downward surface irradiances could be examined. Note that the solid lines between points are interpolations and not a plot of actual data. The plots demonstrate the effect that cloud cover has in increasing the downward longwave irradiances. In the cases where there is cloud cover, Figure 13, the average

downward longwave irradiance value is 240 Wm^{-2} while in the clear sky cases, Figure 12, the average downward longwave irradiance value is 160 Wm^{-2}. This is due to the clouds absorbing upwelling longwave radiation and reemitting it downward, thus increasing the amount of downward longwave irradiance. The large dips in the longwave plot in Figure 14 are places where there was no cloud cover and the surface downward longwave irradiance fell because the reemitting effect of the clouds was absent. To further illustrate this point Figure 15 shows the overcast irradiances indicated with a dashed line plotted over all the longwave cases. The places where the dashed line jumps over the dips is where the downward longwave irradiance decreases because there are no clouds emitting thermal radiation downward. Since there was not as much data for the clear sky cases with measured or modeled downward shortwave irradiance, the effect of cloud cover for the shortwave is not as obvious. It is expected that the surface downward shortwave radiation will decrease as radiation is scattered out of the cloud top and does not reach the surface.

D. DISCUSSION OF UPWELLING SURFACE IRRADIANCES

Having established the best fit values for aerosol and cloud microstructure the model was used to calculate the upward longwave and shortwave surface irradiances. An error

analysis was conducted between the modeled upward and measured upward surface irradiances and the results shown in Table 4.

	Modeled Upward Irradiance
Irradiance	**Correlation Coefficient**
Surface Upward Longwave	0.9864
Surface Upward Shortwave	0.9547
	Average Error (W/m^2)
Surface Upward Longwave	0.4012
Surface Upward Shortwave	-8.267
	Scatter Error (W/m^2)
Surface Upward Longwave	4.3890
Surface Upward Shortwave	6.374
	Total Error (W/m^2)
Surface Upward Longwave	4.4070
Surface Upward Shortwave	10.44

Table 4. Modeled Upward Irradiance Error Analysis.

The modeled upward irradiances are presented in Figures 16 through 18. Upward and downward shortwave irradiance for all cases is shown in Figure 16. Upward and downward longwave irradiance for all cases is shown in Figure 17. Both the shortwave and longwave upward and downward irradiances are plotted together in Figure 18. Note that upward irradiance is positive for ease of comparison with downward values.

The first thing of interest is the larger magnitude of the upwelling longwave surface irradiance as compared to the downward longwave irradiance. This is not unexpected as the ocean underneath the ice was considerably warmer (~ -1.8 C)

than the atmosphere at the surface. Thus it was expected that there would be a net flow of heat from the ocean to the atmosphere. The question was where this extra heat came from. While heat can be conducted through the ice, it is also used to melt the ice. The heat flow through the ice from below does not contribute significantly to the surface heat budget until the ice has melted or thinned considerably. Most of the heat comes from the open ocean leads in the ice pack. This extra heat warms the ice surface and surface air and allows for an increased upward longwave irradiance.

As was seen from the discussion of the effects of clouds, an increase in cloud cover causes the downward longwave irradiance to increase. This in turn warms the surface and as a result there is an increase in the upward longwave irradiance. This can be seen in Figure 17. The measured and modeled upward irradiances follow the trend of the downward irradiance. The large drops in the downward irradiance are places where there are clear sky conditions. In these cases the downward longwave irradiance decreases due to a lack of clouds and so the surface cools and emits less upward longwave irradiance. When overcast conditions occur, the downward longwave irradiance increases, the surface is warmed and the upward longwave irradiance increases. Note also that the shortwave upward irradiance also follows the trend of the

downward shortwave irradiance. This is because the snow-ice surface reflects the shortwave irradiance and so an increase in the amount reaching the surface results in an increase in the amount being radiated upward. Of course, the surface is not a perfect reflector and this is demonstrated by the fact that the upward shortwave irradiance is less than the downward shortwave irradiance. An examination of Figure 16 suggests that the albedo that the model used was not high enough because the measured upward irradiance is always higher than the modeled upward irradiance.

E. SURFACE HEAT FLUX CONTRIBUTIONS AND NET SURFACE HEAT FLUX

For comparison purposes all of the surface heat flux terms are plotted together in Figure 19. Note that for comparison all of the fluxes are positive. It is clear that the latent heat flux is the smallest contributor while the longwave irradiances play the largest role in heat transport. Adding up all of the upward and downward contributions a net surface heat flux was plotted in Figure 20. In this case a positive value means a cooling of the surface. The mean net (upward) heat flux was 77.5 Wm^{-2} at the ice surface. Thus the ocean is losing 77.5 Wm^{-2} to the atmosphere per day averaged between clear sky and overcast conditions. This heat loss is not coming solely through the ice as mentioned earlier but is also being lost through open water leads in the ice field. In

order to better show the importance of all the heat flux terms to the total surface heat budget, Figure 21 shows the average heat flux values plotted over the total period. It is clear that the largest terms in the surface heat budget equation during the austral winter are the longwave terms with the upward longwave being dominant. Factors that affect the longwave irradiances will have the largest effect on the surface heat budget.

Looking at only the dips in Figure 20 which represent overcast days the range is between 0 to 48 Wm^{-2}. This is somewhat larger than measurements made by Andreas and Makshtas (1983) that put surface cooling between 5 and 15 Wm^{-2} on overcast days. If the turbulent fluxes are eliminated and just the net irradiances plotted (Figure 22, bottom dips), the range is between 0 and 20 Wm^{-2} on overcast days. This might indicate that Andreas and Makshtas (1983) did not experience much turbulent heat flux during their experiment or that turbulent heat flux was being advected away from their measuring location. The net heat flux gives an indication of what kind of heat flux is necessary to maintain a constant ice cover. In order for the ice to melt more heat would have to be brought up to the ice-ocean interface from below or more heat would have to be brought down to the surface of the ice from the atmosphere.

In comparing Figures 12 and 20 it is interesting to note that the maxima in the net heat flux occur during clear day periods. This is because during the clear days there is a larger amount of heat that can escape the snow/ice surface. During cloudy days there is a decrease in the net flow because more radiant energy is trapped between the surface and the cloud layer. The clouds can decrease the surface cooling by as much as 140 Wm^{-2} (Figure 20) and bring the net cooling to a near zero value. If warm air were to be advected in or an overturning event in the ocean were to bring up extra heat to the surface, the effect of a stratus layer might be enough to cause a net warming of the surface.

F. DISCUSSION OF EMPIRICALLY DERIVED SURFACE IRRADIANCES

The empirical equations developed by Guest (1996) were used to calculate downward shortwave and longwave irradiance for both the clear sky cases and the overcast cases that were run in STREAMER. The calculated irradiances were then compared with the measured shortwave and longwave irradiances. Using the modeled clear sky irradiances with the marine aerosol optical model and the overcast irradiances with a 2.5 micron droplet size and a 0.05 gm^{-3} water concentration as the best fit modeled irradiance values, the modeled irradiances were compared to the empirical irradiances. The model (STREAMER) performed better than the empirical equations for

the clear sky cases and performed just about the same for the cloudy sky cases. The error analysis performed on the measured and empirically derived irradiances is shown together with the error results of the modeled clear and overcast cases in Table 5.

	Model	Empirical
Correlation Coefficient		
Clear sw	.9536	.9442
Clear lw	.9525	.9016
Overcast sw	.9605	.9326
Overcast lw	.9762	.9677
Average Error (W/m^2)		
Clear sw	1.566	7.767
Clear lw	-2.023	-1.872
Overcast sw	-4.551	1.966
Overcast lw	0.2924	1.108
Scatter Error (W/m^2)		
Clear sw	13.6	14.21
Clear lw	5.487	10.94
Overcast sw	5.627	6.979
Overcast lw	6.852	6.215
Total Error (W/m^2)		
Clear sw	13.69	16.19
Clear lw	5.848	11.10
Overcast sw	7.237	7.25
Overcast lw	6.858	6.313

Table 5. Empirically Derived Irradiance Error Analysis.

The total error values for the clear sky longwave and shortwave irradiances indicates that at least with this data set STREAMER is a better predictor of irradiance. For the overcast case the difference was negligible and both the model and the empirical equations had the same predictive ability. Since there was a reasonable amount of data for the clear sky longwave irradiance comparison and because the total error between the two was not noticeable (5.8 Wm^{-2} for the model and 11.1 Wm^{-2} for the empirical equations), the model does seem to be a better predictor but may not be significantly better. The lack of data for the clear sky shortwave irradiance makes it difficult to say that the difference between the model and the empirical equation is significant. Analysis of additional data might narrow the difference. A weakness in both the model and the empirical equation predictions is that shortwave irradiance is artificially taken to be zero for a solar zenith angle greater than 90 degrees even though common experience shows this to be wrong.

While both the model and the empirical equations give comparable results the empirical equations were derived to produce a minimum amount of error specifically for this particular data set. They could not be used successfully in a different latitude or a radically different physical setting.

The true power of the empirical equations is that they depend on only two variables, the solar zenith angle and the air temperature, both of which are extremely easy to measure in the field. This makes them a very useful tool for estimating the downward surface irradiances without having to have a lot of background information on the structure of the atmosphere.

For comparison purposes the measured, modeled and empirically derived downward irradiances are plotted in Figures 23 through 25. Figure 23 shows all of the data in both the clear sky and overcast sky cases plotted together. Note that the solid lines between points are interpolations and not a plot of actual data. In general the agreement between the modeled, empirical and measured data is quite good. The clear sky irradiances and overcast irradiances are plotted separately in Figures 24 and 25 and the differences from the measured data are a little more apparent.

G. SCIENTIFIC AND OPERATIONAL UTILITY OF STREAMER

As was mentioned earlier, this was not a STREAMER validation study. However, due to the nature of the study the usefulness and accuracy of the model were tested.

The comparisons of the model irradiances with both the measured data and the empirically derived data show that the model can produce excellent results if the proper input

variables are known such as pressure, temperature and moisture profiles and aerosol and cloud properties. If these have to be estimated then the accuracy of the model will be decreased. Empirically derived equations such as the ones developed by Guest (1996) offer comparable accuracy without having to determine all of the input information. Considerable work must go into developing these equations however if they do not already exist.

The greatest use of the model is in its ability to give the user a good understanding of the physical factors which affect the flow of radiation. While the model can be used satisfactorily in the field, it would have to be used in conjunction with shortwave and longwave measured irradiances. These are required to determine the input variables. If the input variables are known, then the model gives excellent results. Difficult to measure variables such as cloud height, cloud thickness, aerosol structure and rawinsonde profiles make empirical equations a more attractive alternative. For this reason the model has its greatest applicability as a scientific research tool and is probably not suited for operational and field use.

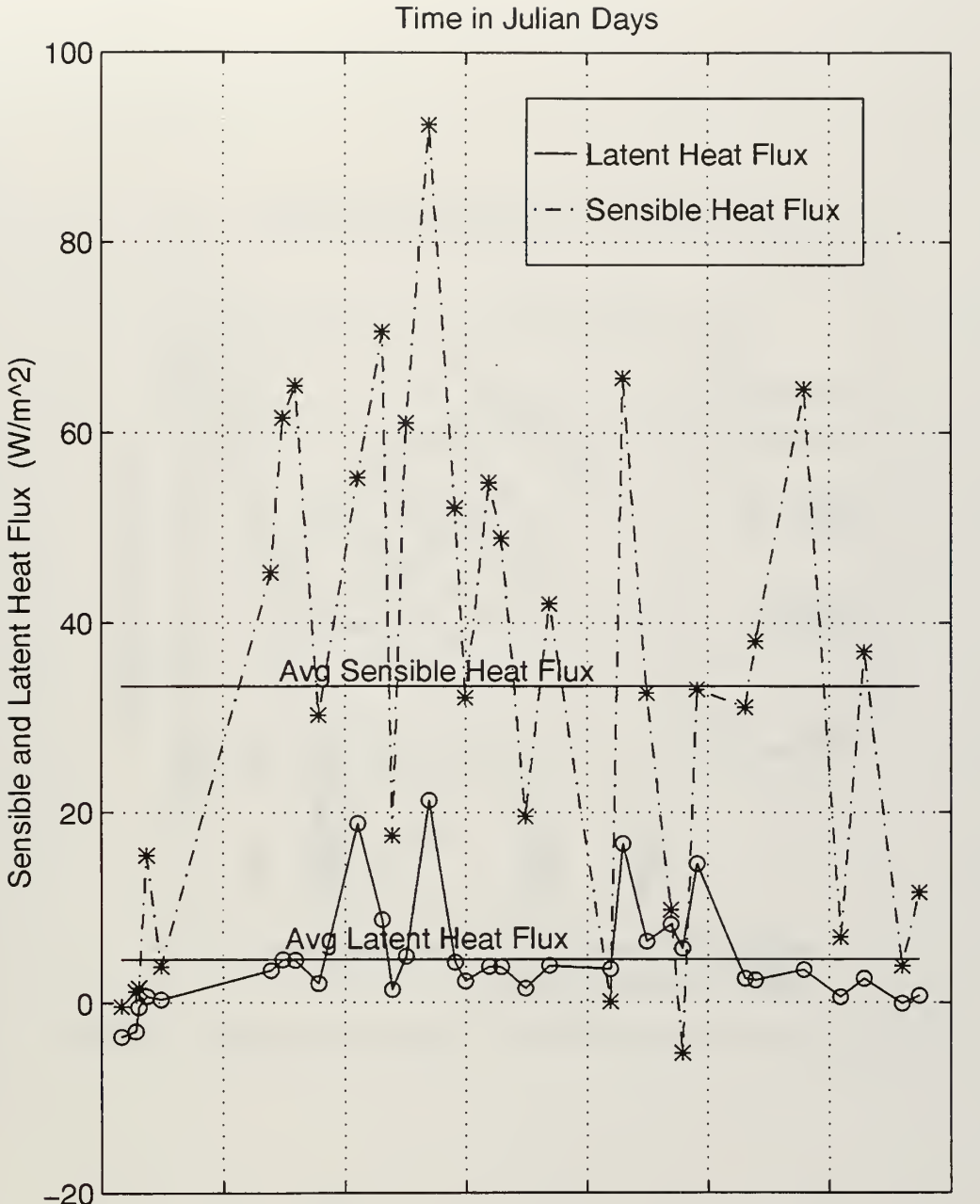

Figure 5. Area Averaged Turbulent Heat Fluxes.

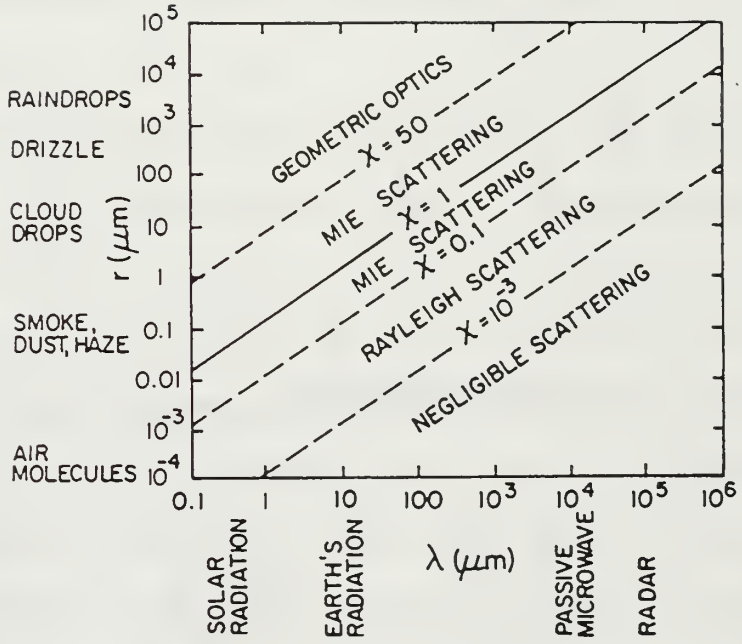

Figure 6. Scattering Regimes (from Kidder and Vonder Haar, 1995).

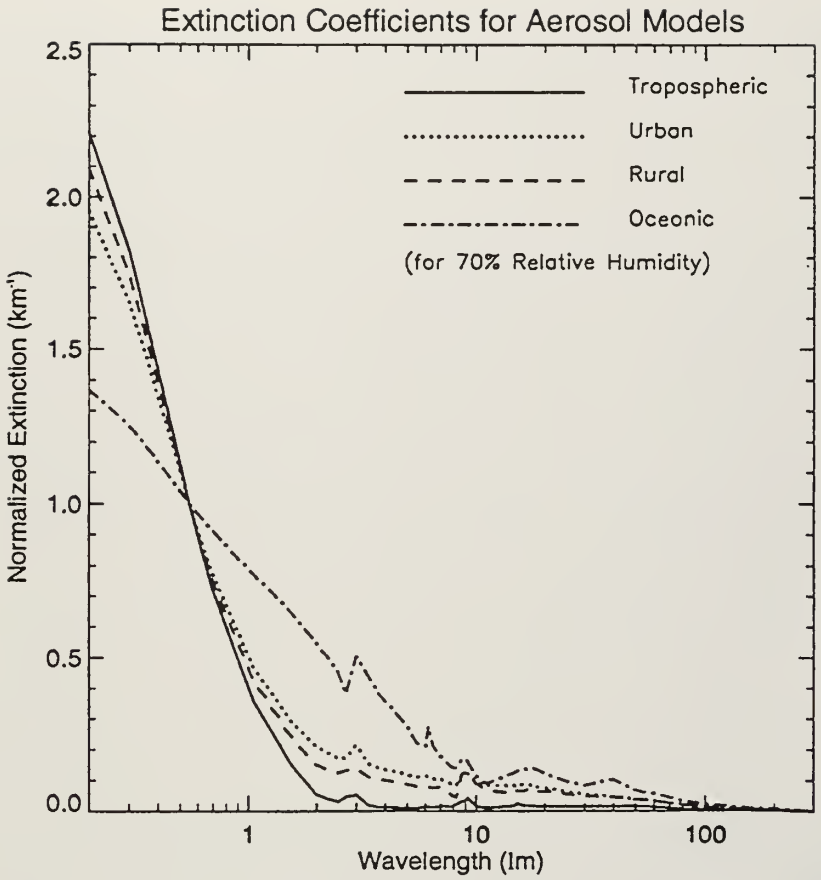

Figure 7. Extinction Coefficient versus Wavelength (from Key, 1996).

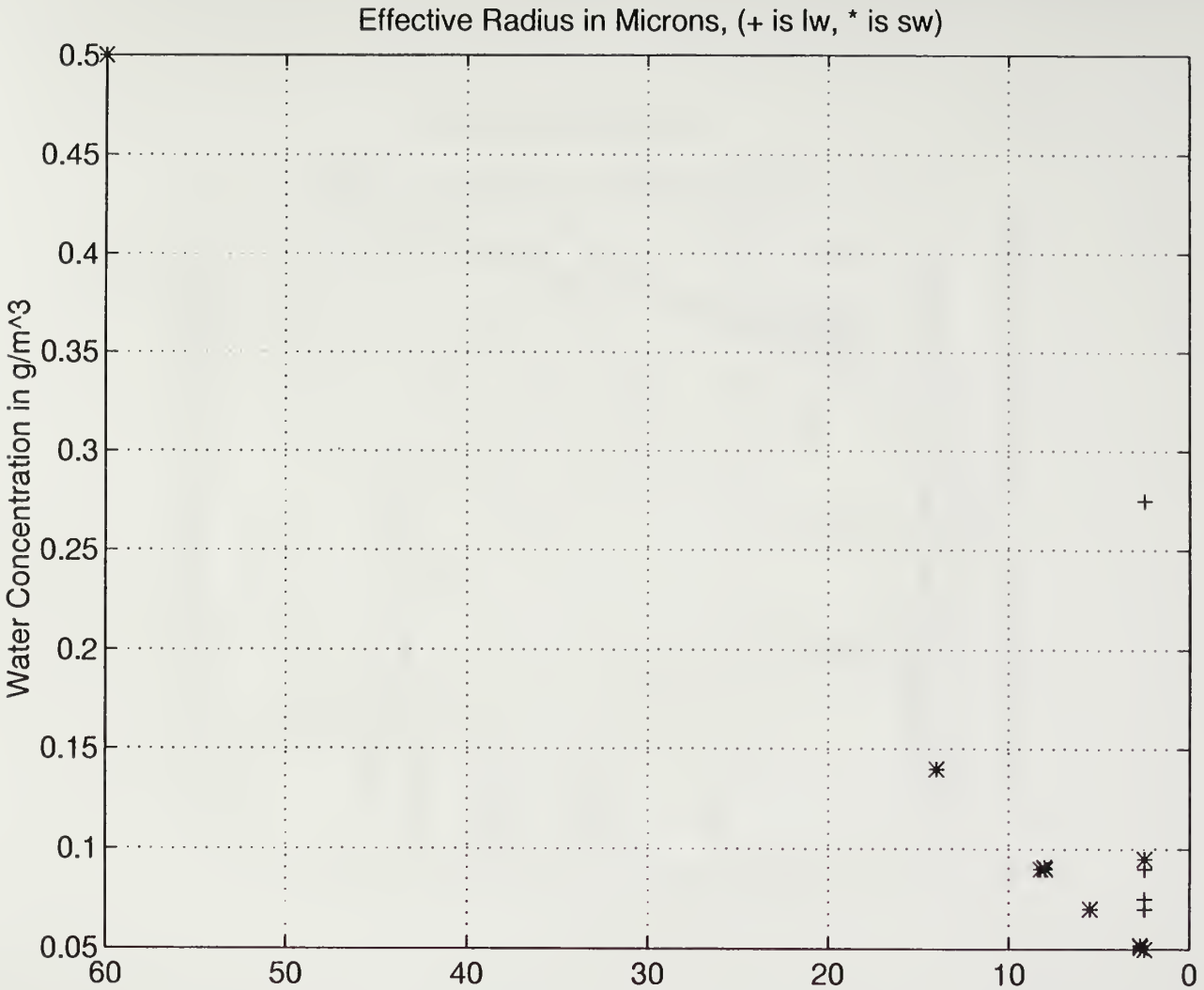

Figure 8. Drop Effective Radius vs. Water Concentration for Overcast Cases.

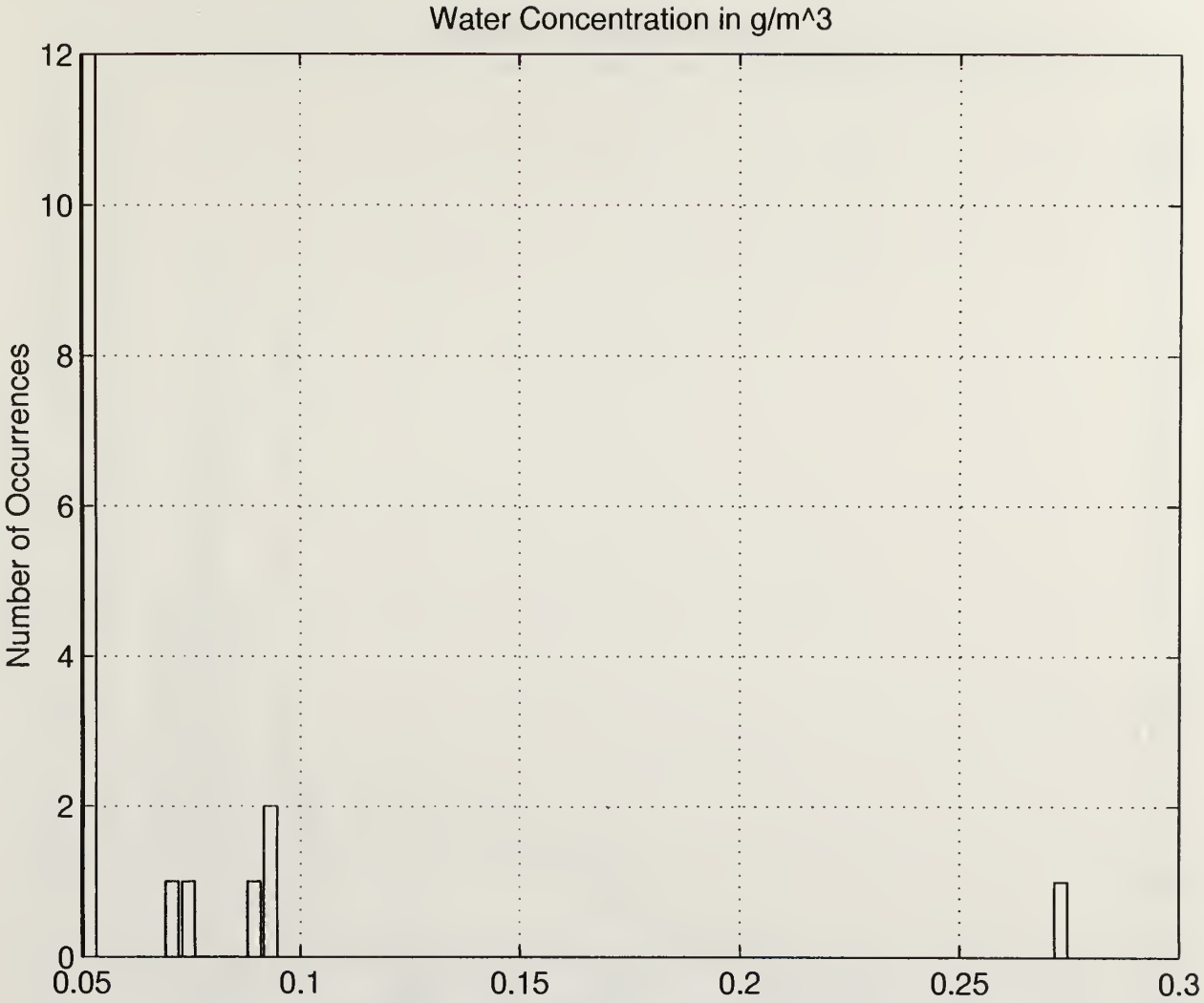

Figure 9. Longwave Histogram of Water Concentrations at Effective Radius of 2.5 microns.

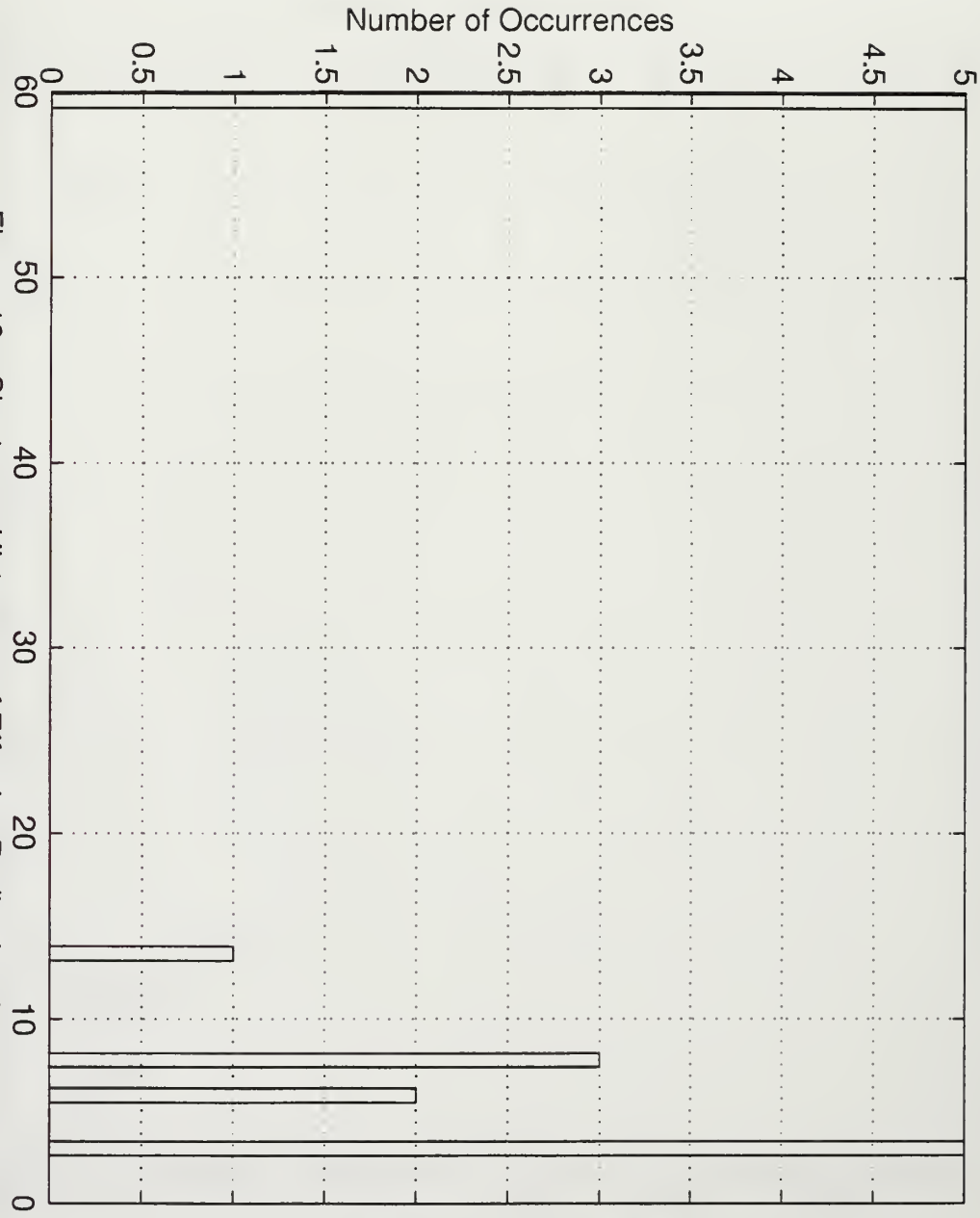

Figure 10. Shortwave Histogram of Effective Radius in microns.

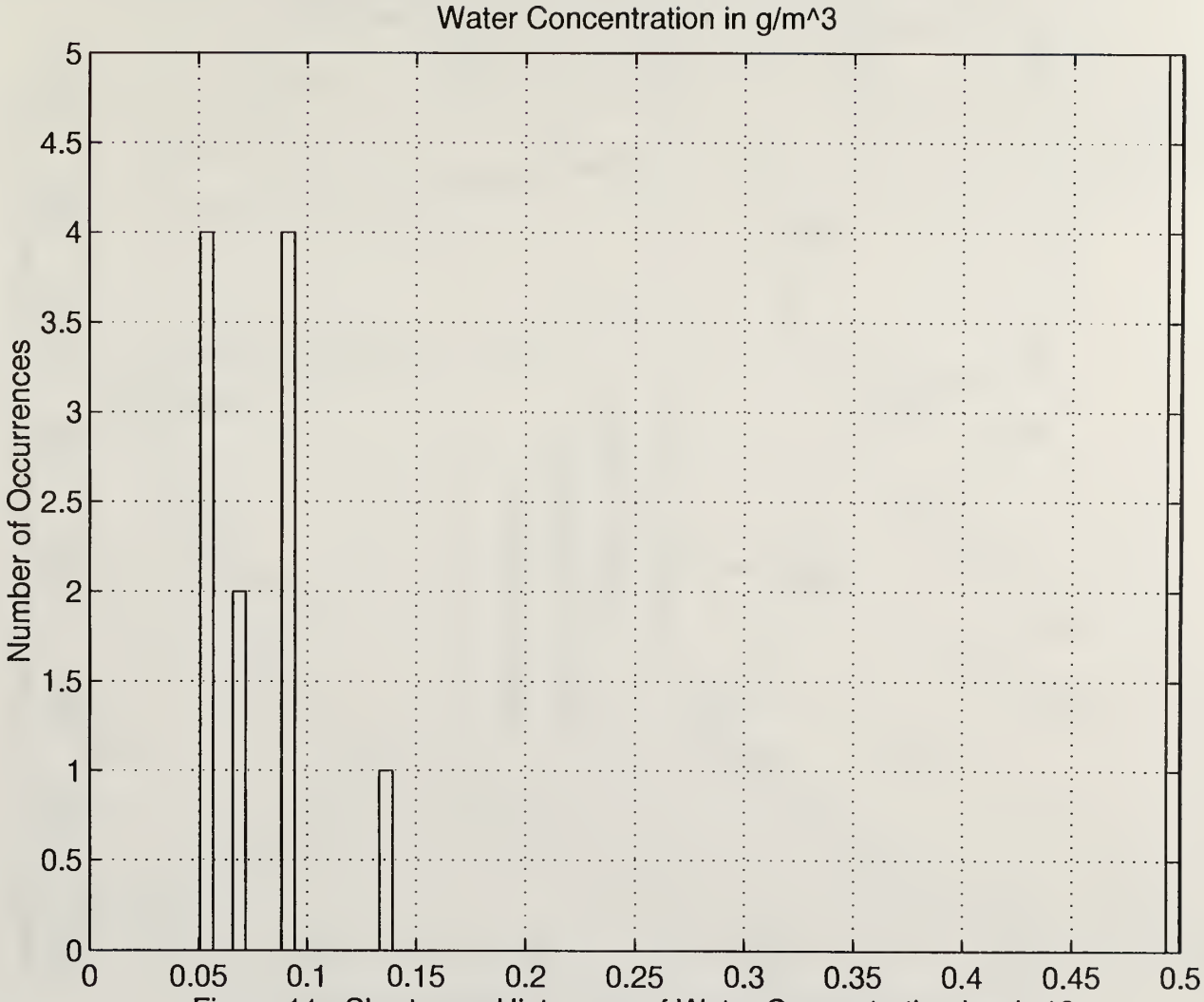

Figure 11. Shortwave Histogram of Water Concentration in g/m^3.

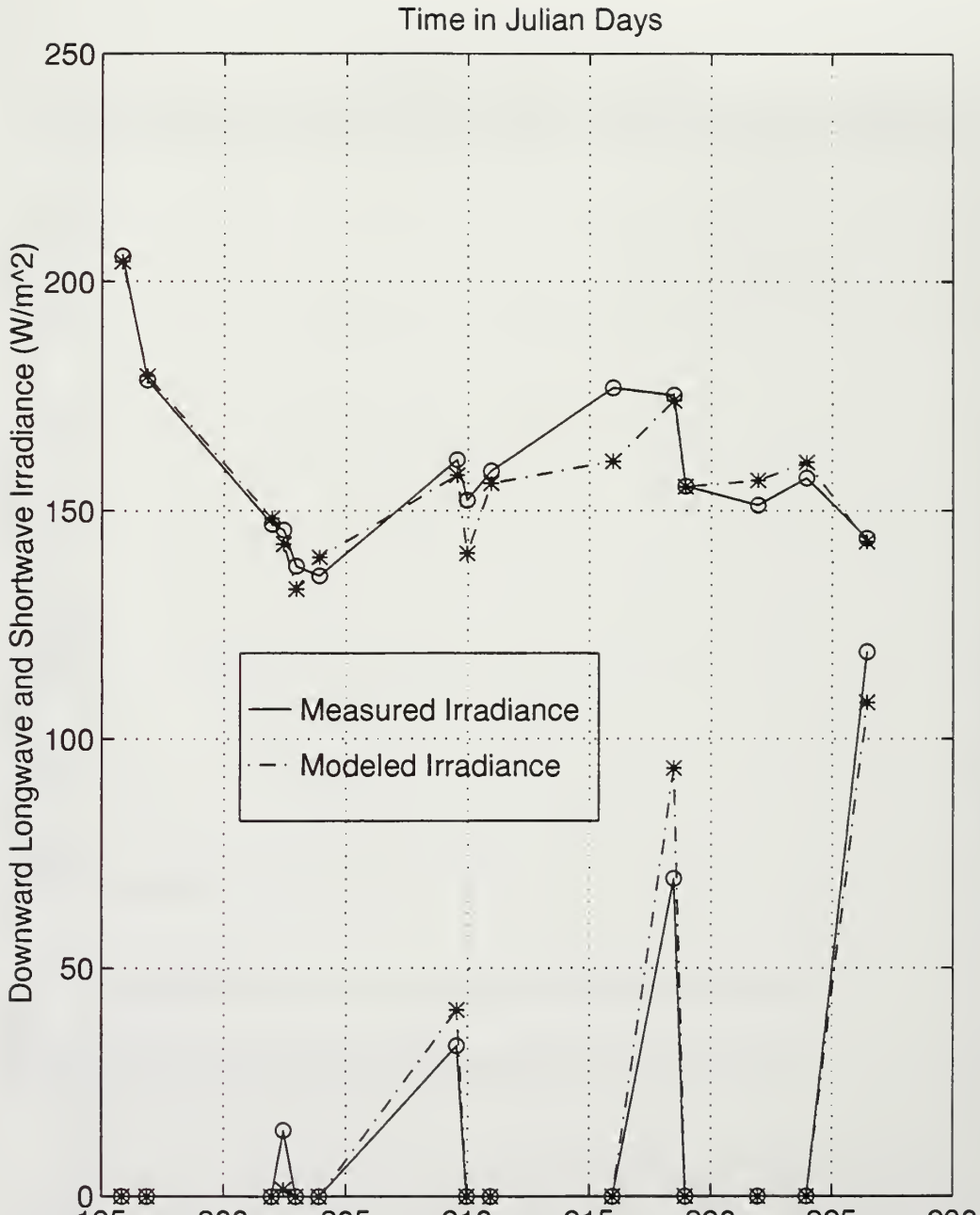

Figure 12. Measured and Modeled Irradiances for Clear Cases.

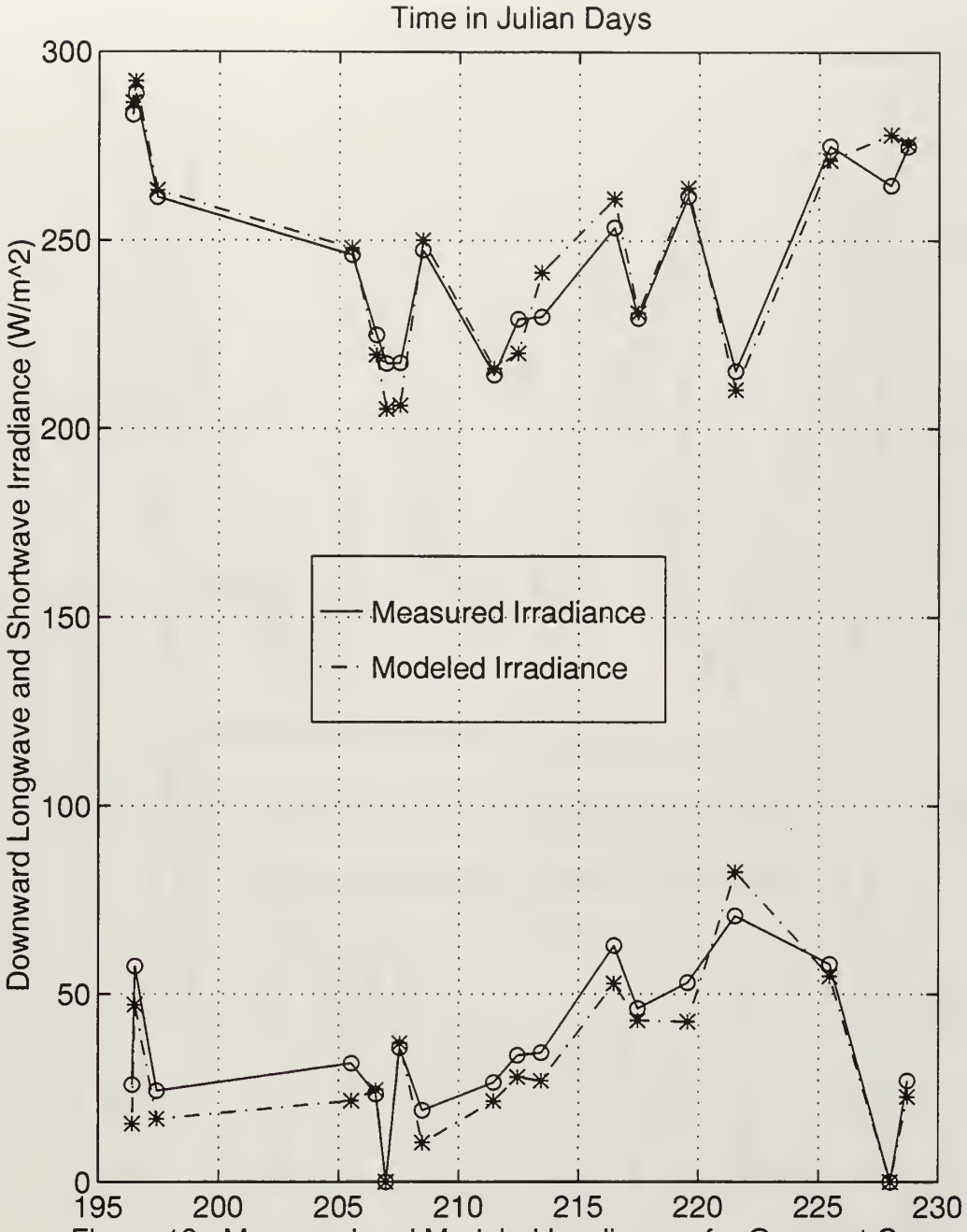

Figure 13. Measured and Modeled Irradiances for Overcast Cases.

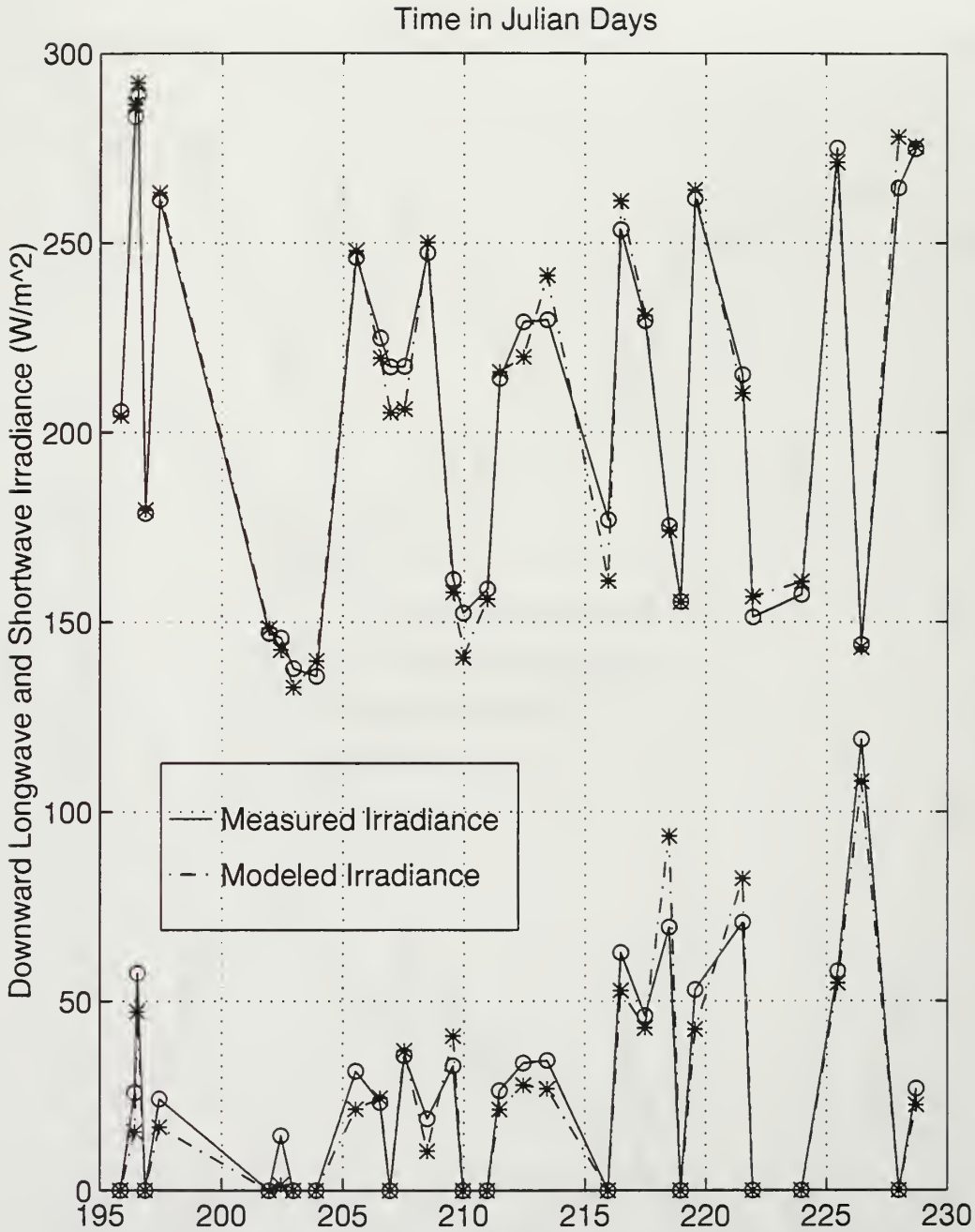

Figure 14. Measured and Modeled Irradiances for All Cases.

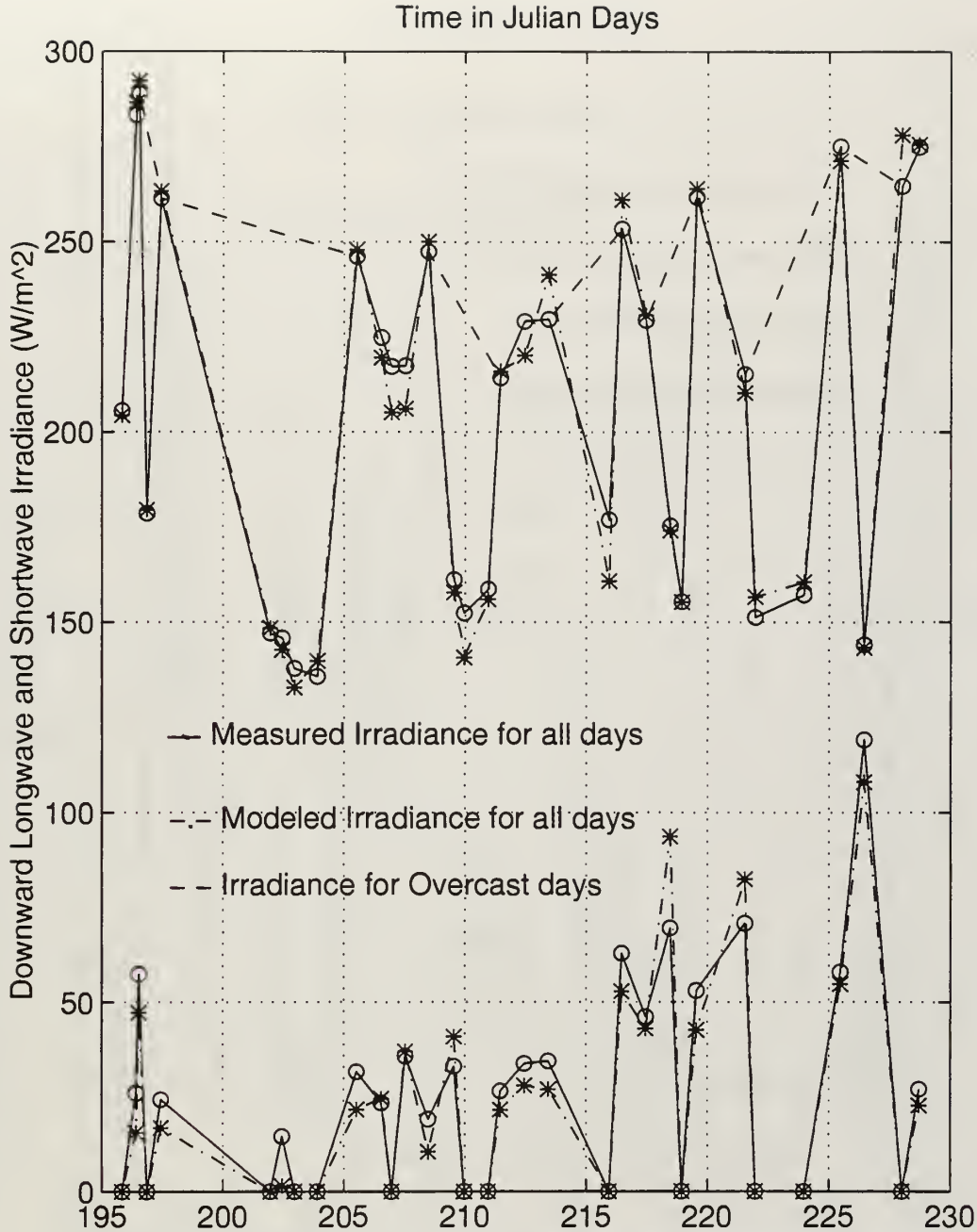

Figure 15. Effects of Clouds on Downward Surface Irradiances.

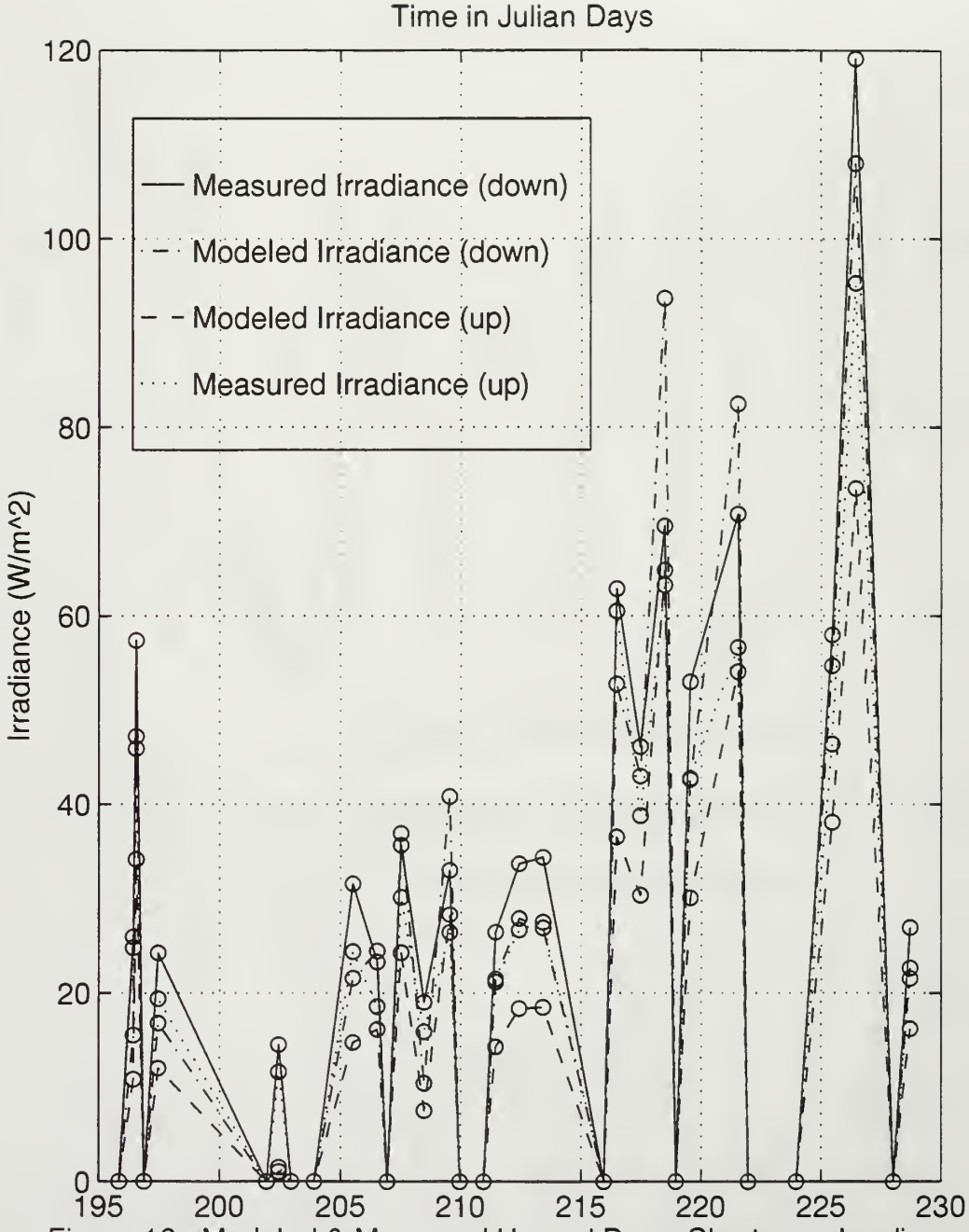

Figure 16. Modeled & Measured Up and Down Shortwave Irradiances.

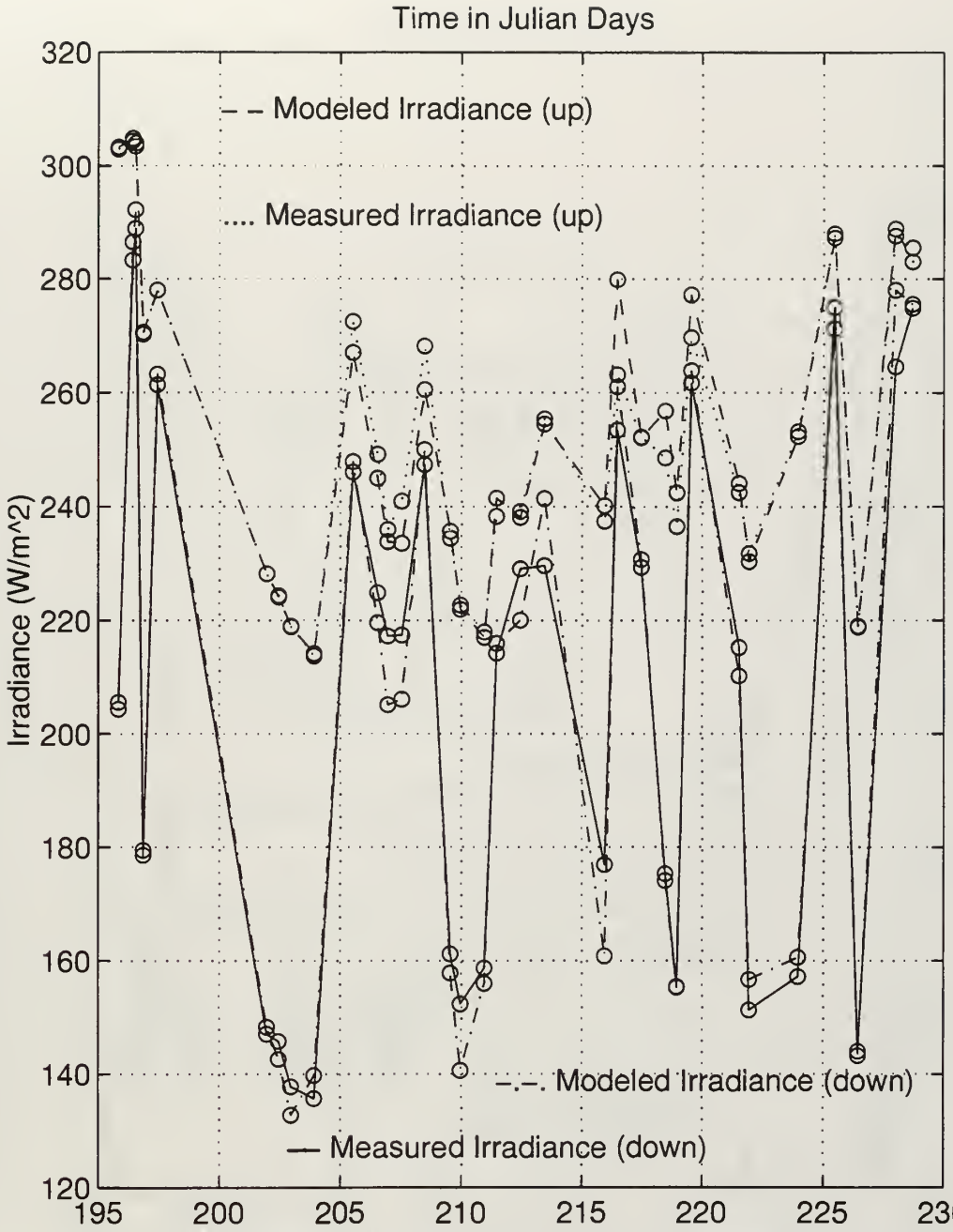

Figure 17. Modeled & Measured Up and Down Longwave Irradiances.

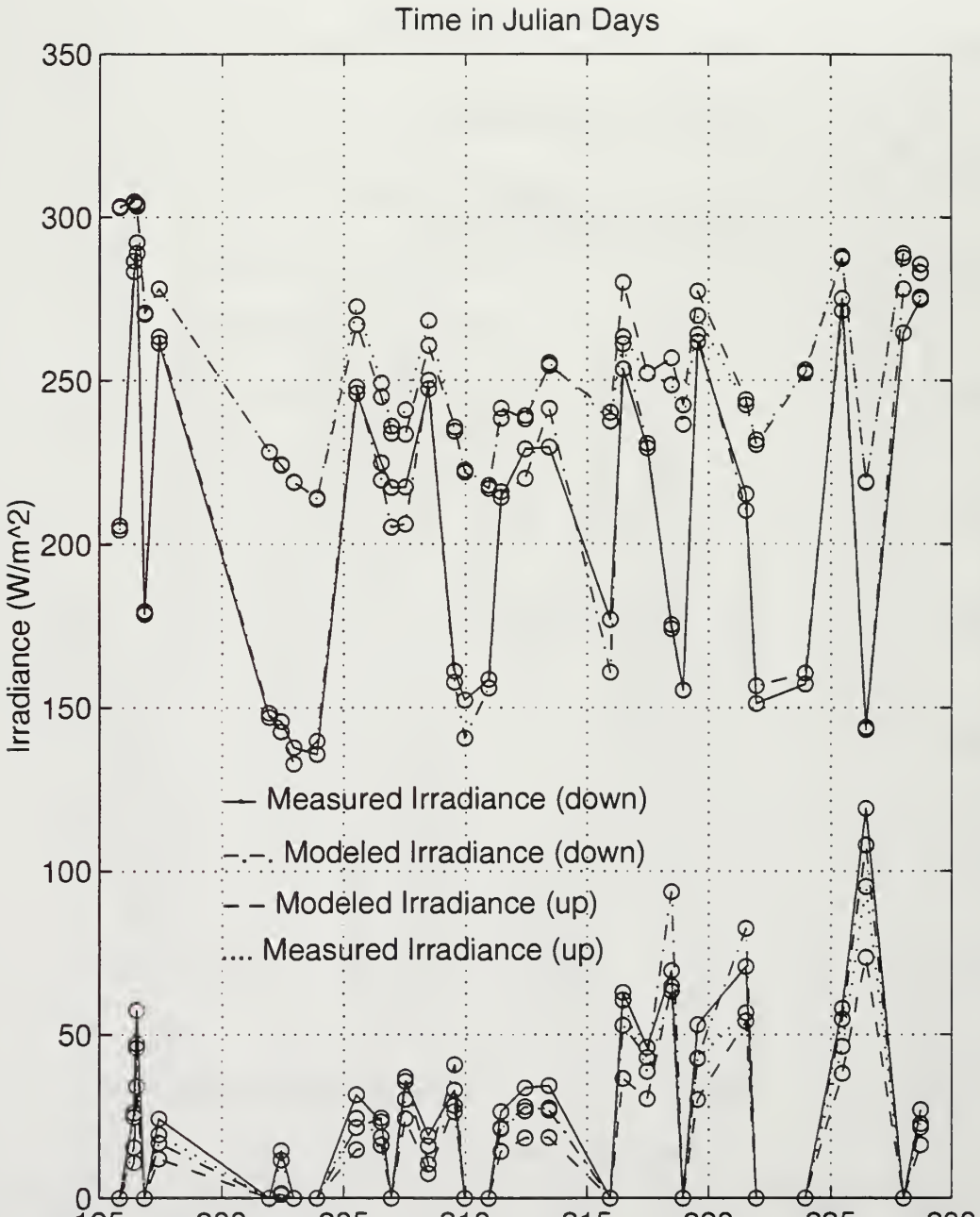

Figure 18. Modeled & Measured Short and Longwave Irradiances.

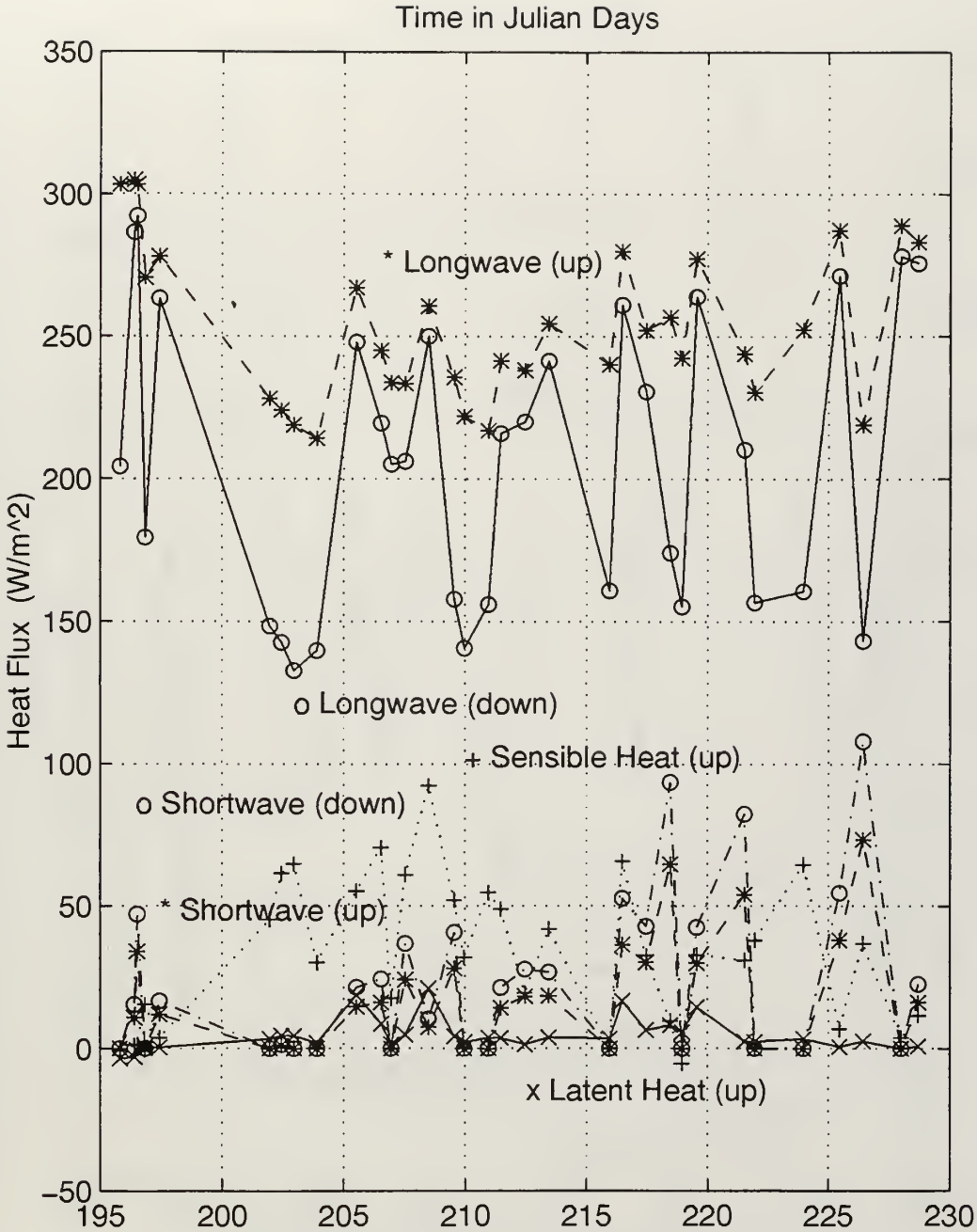

Figure 19. Surface Heat Flux Contributions.

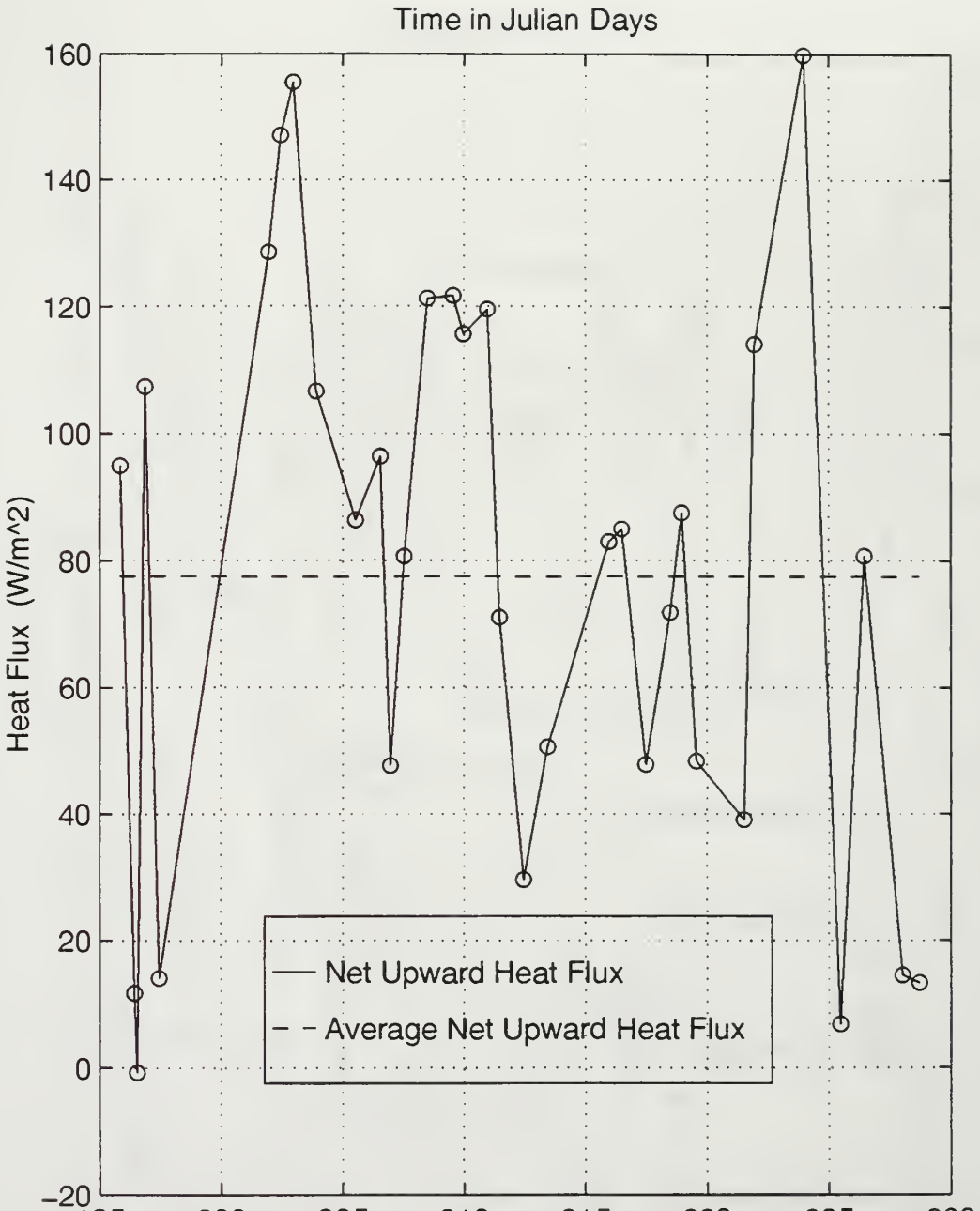

Figure 20. Net Surface Heat Flux (Upward).

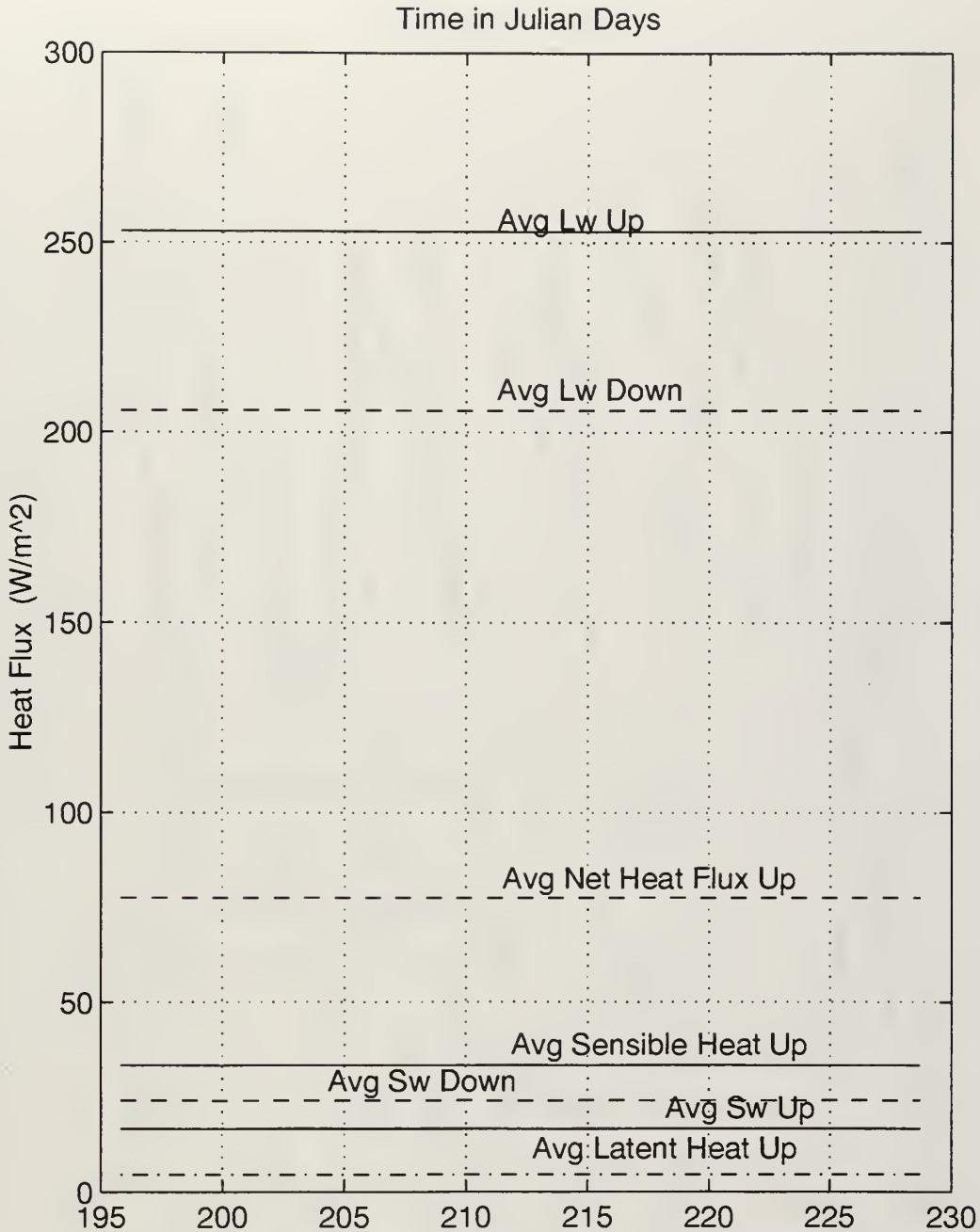

Figure 21. Average Surface Heat Flux Contributions.

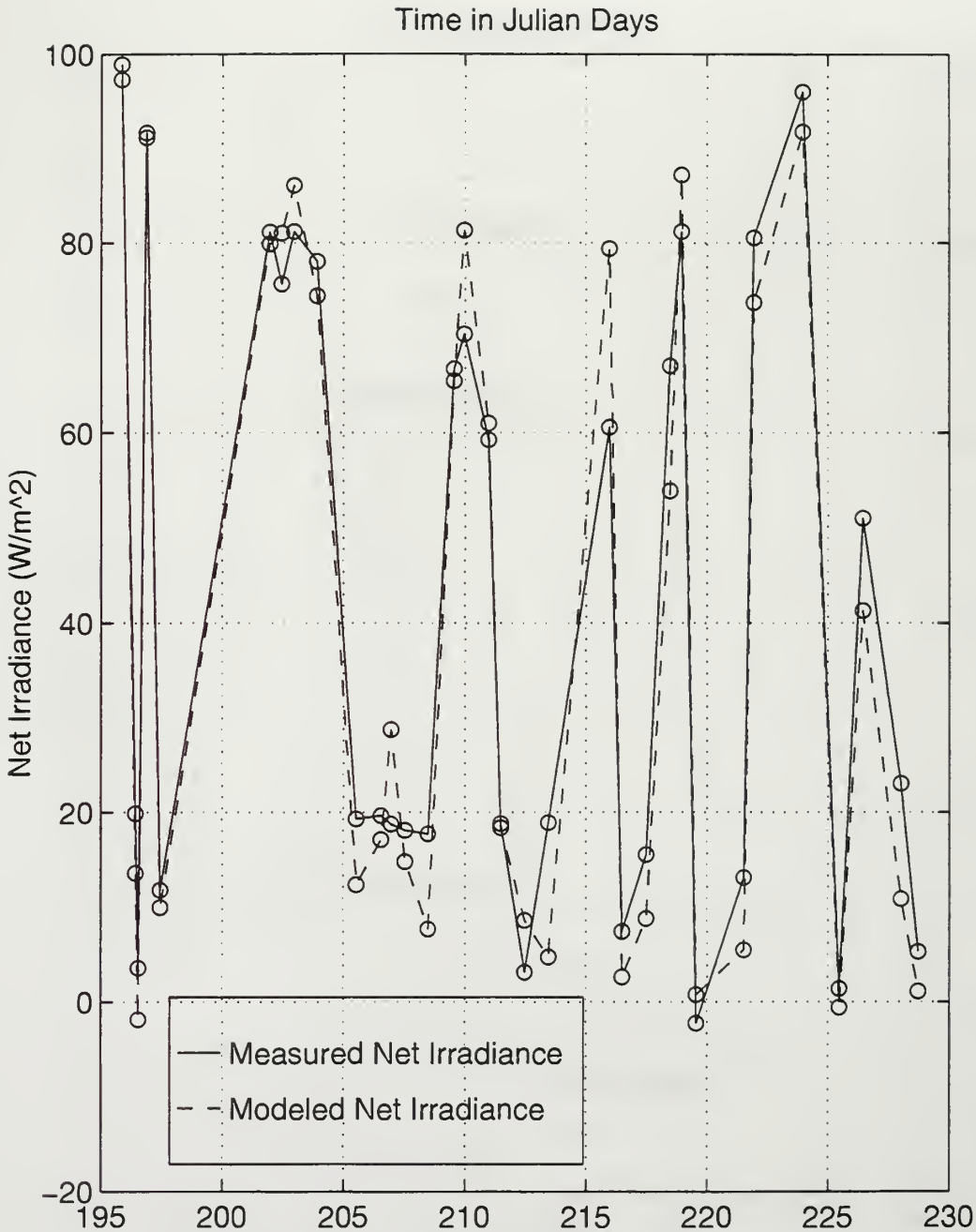

Figure 22. Net Measured & Modeled Irradiance.

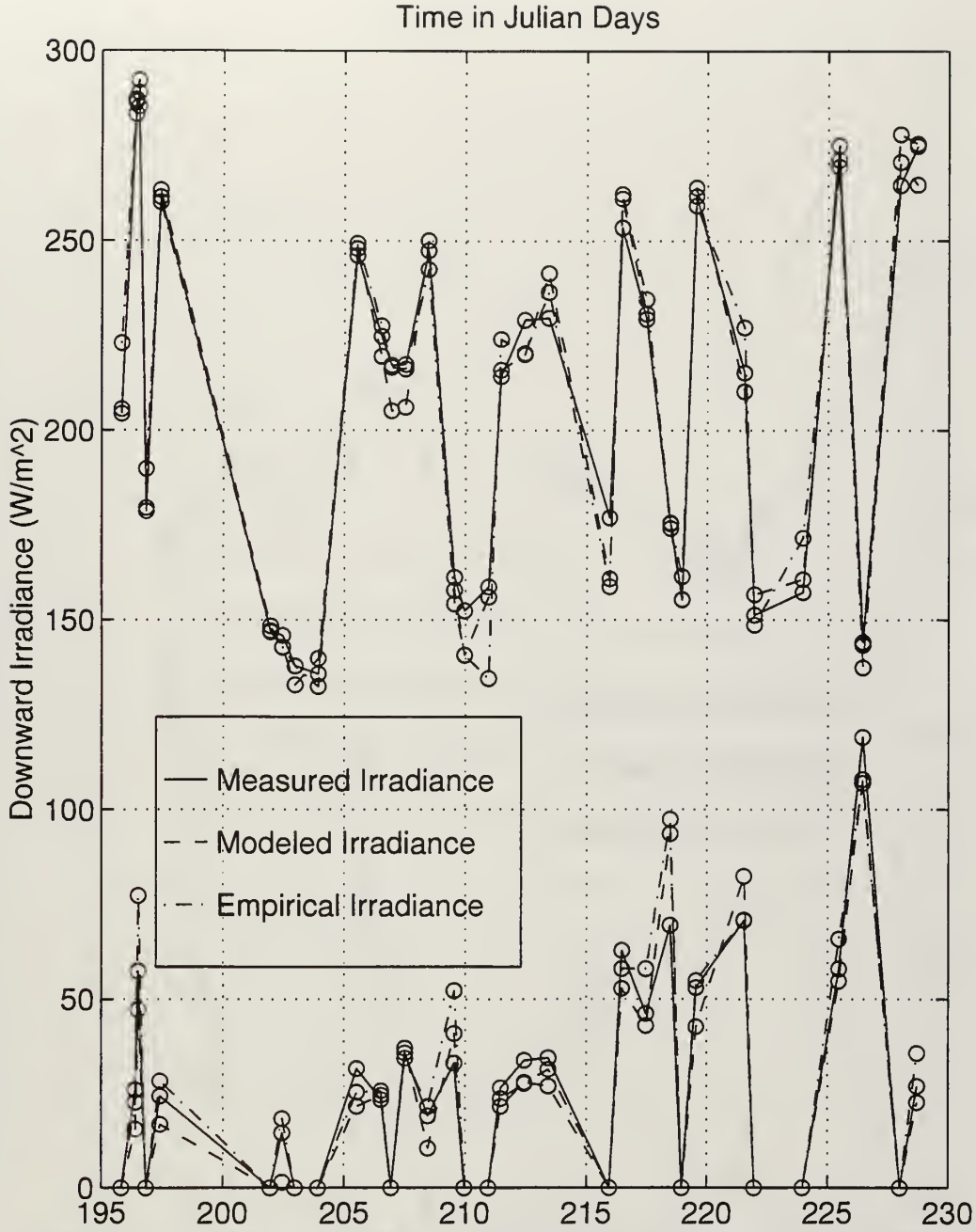

Figure 23. Measured, Modeled & Empirical Irradiances for All Cases.

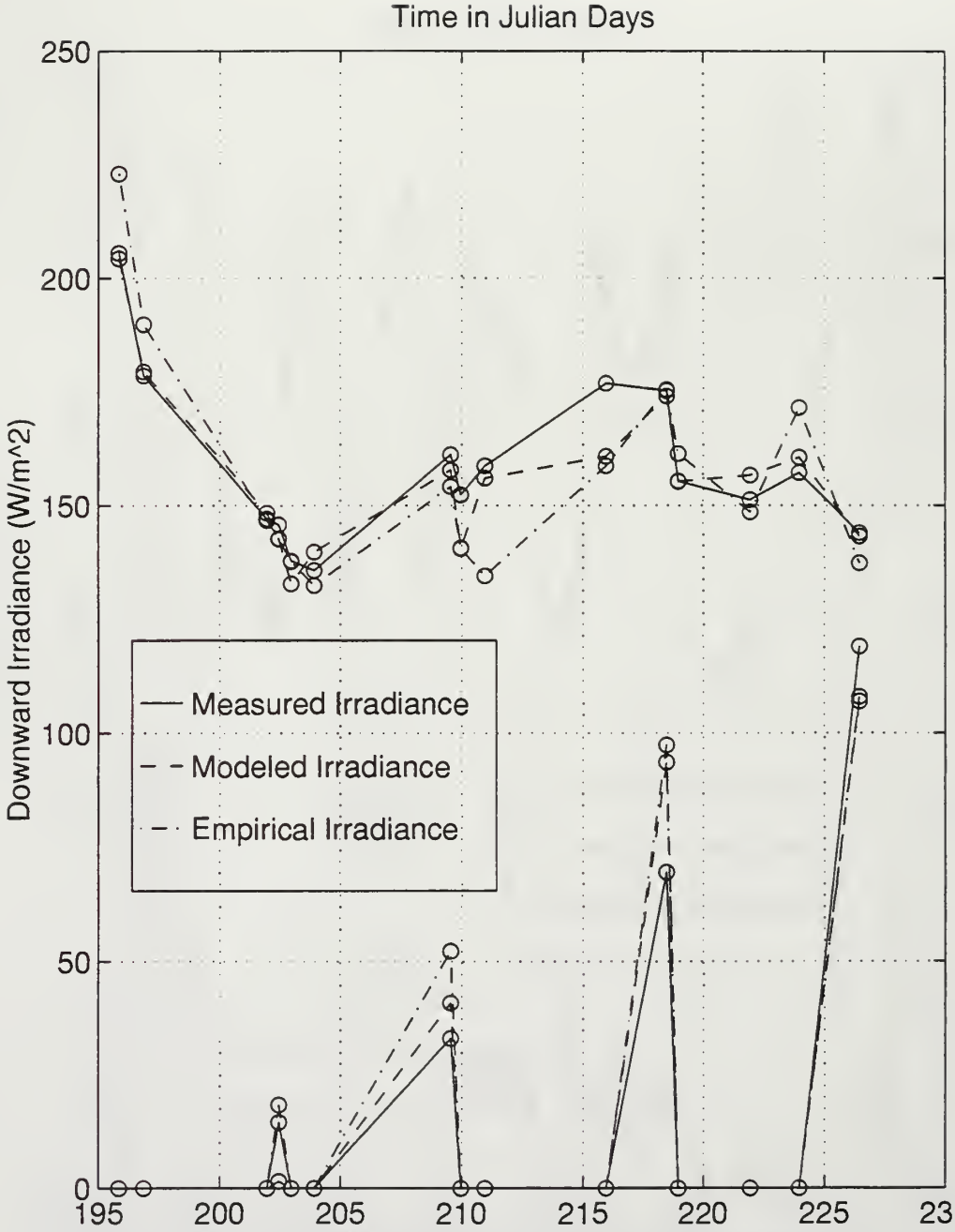

Figure 24. Measured, Modeled & Empirical Irradiances for Clear Cases.

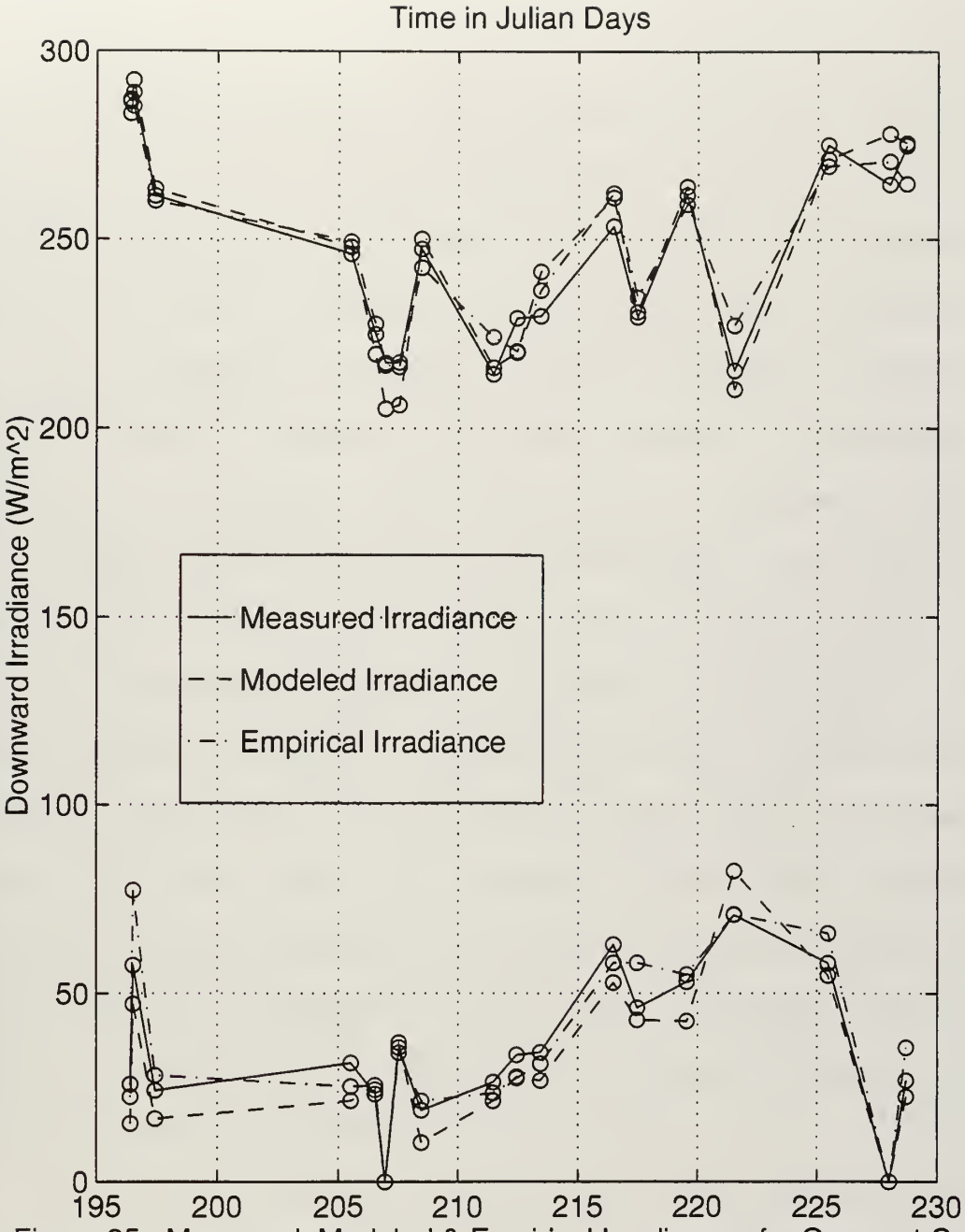

Figure 25. Measured, Modeled & Empirical Irradiances for Overcast Cases.

VII. SUMMARY

The surface heat budget of the Weddell Sea air-ice interface is dominated by the longwave radiation terms during the austral winter. During this time the upwelling longwave irradiance is the largest term in the surface heat budget and represents a net cooling of the air-ice-ocean interface.

The longwave irradiance is most strongly affected by cloud cover. Effects on the longwave irradiance by atmospheric aerosols are negligible. Aerosols have a significant effect on shortwave irradiances. The most likely aerosol structure in the Weddell Sea air appears to be quite similar to marine aerosol profiles in that the aerosol concentration builds to a maximum aloft with a minimum at the surface. The total column optical depth appears to be very close to 0.08. This is slightly higher than previously recorded seasonal means but might possibly be due to high level Polar Stratospheric Clouds that routinely form in the austral winter or the presence of stirred up snow or ice crystals from the surface.

The microstructure of the stratus that appears over the Weddell Sea is most likely composed of very small droplet sizes, around 2.5 microns, with a very low water concentration, around 0.05 gm^{-3}. These stratus clouds have a

major impact on both the shortwave and longwave terms of the surface heat budget. The clouds can act to reduce surface cooling by as much as 160 Wm^{-2} and can actually act to reverse surface cooling. If warm air were to be advected in or an overturning event in the ocean were to bring up extra heat to the surface, the effect of a stratus layer might be enough to cause a net warming of the surface.

STREAMER, a radiative transfer model, can be used to predict surface irradiances with great accuracy if profiles of atmospheric temperature, moisture, pressure and atmospheric aerosol and cloud microstructure parameters are known. The model gave excellent agreement with measured irradiances once key parameters were determined. If these parameters cannot be obtained, then empirical equations specifically developed for the Weddell Sea in Antarctica provide comparable results and require only surface temperature and solar zenith angle. These parameters can be measured easily and inexpensively. STREAMER is an excellent research tool and could have unlimited applications for operational or field use if the necessary model parameters are known or easily measured.

LIST OF REFERENCES

Andreas, E.L., and A.P. Makshtas, Reports of the U.S.-U.S.S.R. Weddell Polynya Expedition, October-November 1981: Vol. 7, Surface-level meteorological data. *Special Rept. 83-14,* U.S. Cold Regions Research and Engineering Laboratory, Hanover, N.H., 32 pp., 1983.

Andreas, E.L., A theory for the scalar roughness and the scalar transfer coefficients over snow and sea ice, *Boundary Layer Meteorol.*,38,159-184,1987.

Curry, J.A. and E.E. Ebert, Annual cycle of radiation fluxes over the Arctic Ocean: sensitivity to cloud optical parameters, *J. Climate,* 5, 1267-1280, 1992.

Curry, J.A., F.G. Meyer, L.F. Radke, C.A. Brock and E.E. Ebert, Occurrence and characteristics of lower tropospheric ice crystals in the Arctic, *International J. Clim.,* 10, 749-764, 1990.

Ebert, E.E., and J.A. Curry, A parameterization of ice clouds optical properties for climate models, *J. Geophys. Res.,97(D4),3831-3836, 1992.*

Ellingson, R.G., J. Ellis, and S. Fels, The intercomparison of radiation codes used in climate models: longwave results, *J. Geophys. Res.,* 96(D5),8929-8953, 1991.

Feigelson, E.M., *Radiation in a Cloudy Atmosphere,* D. Reidel Publishing Co., Dordrecht, The Netherlands, 292 pp., 1984.

Garratt, J.R., *The Atmospheric Boundary Layer,* Cambridge University Press, Cambridge, 316 pp., 1992.

Gordon, A.L., Two stable modes of Southern Ocean winter stratification in *Deep Convection and Deep water Formation in the Oceans*, P.C. Chu and J.C. Gascard, eds., Elsevier Oceanography Series, 57, New York, 17-35,1991.

Gow and Tucker, CRREL Monograph 91-1, 24-28,CRREL, Hanover, 1991.

Guest, P.S., and K.L. Davidson, Factors affecting variations of snow surface temperature and air temperature over sea ice in winter in *The Polar Oceans and Their Role in Shaping the Global Environment*, 85, 435-442, 1994.

Guest, P.S., K.L. Davidson, J.E. Overland and P.A. Frederickson, Atmosphere-Ocean interaction in the marginal ice zones of the nordic seas, *Arctic Oceanography: Marginal Ice Zones and Continental Shelves Coastal and Estuarine Studies*, 49, 51-95, 1995.

Guest, P.S., Surface radiation conditions in the Eastern Weddell Sea during winter, Submitted to *J. Geophys. Res., (Oceans)*, 1996.

Hu, Y.X., and K. Stamnes, An accurate parameterization of the radiative properties of water clouds suitable for use in climate models, *J. Climate*, 6(4),728-742, 1993.

Jaenicke, R., Tropospheric Aerosols, *Aerosol-Cloud-Climate Interactions*, P. V. Hobbs, ed., Academic Press, New York, 233 pp., 1993.

Key, J., *STREAMER User's guide*, Technical *Report 96-01*, Department of Geography, Boston University,75 pp., 1996.

Kidder, S.Q., and T.H. Vonder Haar, *Satellite Meterology, An Introduction*, Academic Press, New York, 466 pp., 1995.

Liou, K.N., *Radiation and Cloud Processes in the Atmosphere*, Oxford Monographs on Geology and Geophysics, 20,Oxford University Press, 487 pp., 1992.

McCormick, M.P., Wang, P.H., and L.R. Poole, Stratospheric Aerosols and Clouds in *Aerosol-Cloud-Climate Interactions,* P.V. Hobbs, ed., Academic Press, New York, 233 pp., 1993.

McPhee, M.G.,S. Ackley, P. Guest, B. Huber, D. Martinson, J.Morison, R. Muench, L. Padman, and T. Stanton, The Antarctic zone flux experiment, *Mon. Wea. Rev.,* 77,1221-1232, 1996.

Paltridge, G.W., and Platt, C.M.R., Radiative Processes in Meterology and Climatology in *Developments in Atmospheric Science 5,* Elsevier Scientific Publishing Co., New York, 318 pp., 1976.

Rogers, R.R., and Yau, M.K., *A short Course in Cloud Physics,* Pergamon, New York, 293 pp., 1989.

Schlesinger, M. And J. Mitchell, Model projections of the equilibrium climatic response to increased carbon dioxide in *the Potential Climatic Effects of Increasing Carbon Dioxide,* United States Dept. of Energy, DOE/ER-0237, 81-148, 1985.

Stamnes, K., S.C. Tsay, W. Wiscombe, and K. Jayaweera, Numerically stable algorithm for discrete-ordinate-method radiative transfer in multiple scattering and emitting layered media, *Appl. Opt.*,27,2502-2509, 1988.

Stull, R.B., *An Introduction to Boundary Layer Meteorology,* Kluwer Academic Publishers, Dordrecht, The Netherlands, 666 pp., 1988.

Toon, O.B., C.P. Mckay, and T.P. Ackerman, Rapid calculation of radiative heating rates and photodissociation rates in inhomogeneous multiple scattering atmospheres, *J. Geophys. Res.,* 94(D13),16287-16301, 1989.

Tsay, S.C., K. Stamnes and K. Jayaweera, Radiative energy budget in the cloudy and hazy Arctic. *J. Atmos. Sci.*,46,1002-1018, 1989.

Tsay, S.C., K. Stamnes and K. Jayaweera, Radiative transfer in stratified atmospheres: development and verification of a unified model, *J. Quant. Spectrosc. Radiative. Transfer,*43,133-148, 1990.

Weller, M. and V. Leiterer, Land Based Optical Depth Measurements, *Contrib. Atmos. Phys,* 61, 1-9, 1988.

Wiscombe, W.J., Radiative Fluxes in a Cloudy Atmosphere--Effects of Drop Size Distribution Variability and of Using the Delta-Eddington Approximation in *Radiation in the Atmosphere,* edited by H.J. Bolle, Science Press, Princeton, 630 pp., 1977.

Yamanouchi, T., and J. B. Orbaek, Comparative study of the surface radiation budget at Ny-Alwsund, Svalbard and Syowa Station, Antarctica, 1987 in *Proc. NIPR Symp. Polar Meteorol. Glaciol.,*9, 118-132, 1995.

INITIAL DISTRIBUTION LIST

No. Copies

1. Defense Technical Information Center.....2
   8725 John J. Kingman Rd., STE 0944
   Ft. Belvoir, Virginia 22060-6218

2. Dudley Knox Library.....2
   Naval Postgraduate School
   411 Dyer Rd.
   Monterey, California 93943-5101

3. Chairman (Code MR/Wx).....1
   Department of Meteorology
   Naval Postgraduate School
   Monterey, California 93943-5000

4. Chairman (Code OC/Bk).....1
   Department of Oceanography
   Naval Postgraduate School
   Monterey, California 93943-5000

5. Prof. Peter S. Guest (Code MR/Gt).....1
   Department of Meteorology
   Naval Postgraduate School
   Monterey, California 93943-5000

6. Prof. Roland W. Garwood (Code OC/Gd).....1
   Department of Oceanography
   Naval Postgraduate School
   Monterey, California 93943-5000

7. LCDR Eugene P. Tramm.....3
   5223 Heming Avenue
   Springfield, Virginia 22151